Measurements of ABB's Prototype Fast Charging Station for Electric Vehicles

A contribution towards standardized models for voltage and transient stability analysis

Master's thesis in Electric Power Engineering

DANIEL ANDERSSON
DAVID CARLSSON

Department of Energy and Environment
Division of Electric Power Engineering
CHALMERS UNIVERSITY OF TECHNOLOGY
Gothenburg, Sweden 2012
Master's thesis

MASTER'S THESIS IN ELECTRIC POWER ENGINEERING

Measurements of ABB's Prototype Fast Charging Station for Electric Vehicles

A contribution towards standardized models for voltage and transient stability analysis

DANIEL ANDERSSON
DAVID CARLSSON

Department of Energy and Environment
Division of Electric Power Engineering
CHALMERS UNIVERSITY OF TECHNOLOGY

Gothenburg, Sweden 2012

Measurements of ABB's Prototype Fast
Charging Station for Electric Vehicles
A contribution towards standardized models
for voltage and transient stability analysis
DANIEL ANDERSSON
DAVID CARLSSON

Master's thesis
ISSN 1652-8557
Department of Energy and Environment
Division of Electric Power Engineering
Chalmers University of Technology
SE-412 96 Gothenburg
Sweden
Telephone: +46 (0)31-772 1000

Cover:
Fast charging of Citroën Z-zero with ABB prototype fast charging station in Agnesberg, Sweden

Chalmers Reproservice
Gothenburg, Sweden 2012

Measurements of ABB's Prototype Fast
Charging Station for Electric Vehicles
A contribution towards standardized models
for voltage and transient stability analysis
Master's thesis in Electric Power Engineering
DANIEL ANDERSSON
DAVID CARLSSON
Department of Energy and Environment
Division of Electric Power Engineering
Chalmers University of Technology

Abstract

In this study, measurements on a prototype CHAdeMO fast charger, ABB PCS DCFC fast charger, with rating of 50kW (125A DC) is investigated. The scope is on the whole system: electric grid, converter and battery with focus on how charging is affected by battery state of charge (SOC), temperature and ambient temperature. A comparison between fast charging with DC and normal charging with 10A AC is also performed.

The output current is limited of the battery temperature during fast charging. Below approximately 10^oC the charging current is 25A and between approximately 10 to 20^oC the charging current is 50A, above 20^oC at rated current of 125A is used.

The efficiency of the fast charger is 90% at 50kW DC and decreases to 50% at 2kW DC. The efficiency of AC charging, using the on-board charger, is approximately 95% and the charging time is 8h instead of 1.5h with DC charging. Using the fast charger to charge the battery to 80% and then use AC charging is suggested as a charging strategy in coming standards.

The fast charger impact the electric grid by causing a 10V voltage dip at full power (50kW DC) but reduces low order harmonics when operating. At standby the fast charger consumes 400W, corresponding to fully charge 219 batteries of 16kWh in a year. The option to use the charger as a STATCOM or filter even when no car is connected in order to improve power quality is suggested.

Keywords: ABB, CHAdeMO, Electric Vehicle, Fast charging, Range anxiety, Transient stability

Acknowledgements

This work has been carried out at the Department of Energy and Environment at Chalmers University of Technology. We offer our gratitude to our supervisor Patrik Svedberg at HRM Engineering, who has supported us through this thesis and Gordon Strömfelt as an engaged coordinator of the project also working for HRM Engineering. We also offer our gratitude to our examiner Hector Zelaya De La Parra for great support and many interesting ideas. In our daily work we have received great support from Magnus Ellsén regarding measurement equipment and Torbjörn Thiringer for technical expertise. We are sincerely grateful to Hans-Olof Nilsson at H-O Enterprise for giving us the opportunity to have access to electric vehicle and fast charging station and Fredrik Persson at Göteborg Energi for his support during the measurements.

We also want to thank Test Site Sweden for the invitation and financial support to attend North Sea Electric Network first international workshop regarding ”experience and future of electric vehicle fast charging” in Hamburg 15 March 2012 which gave valuable input. Finally, our gratitude to Hans-Olof Nilsson for registration fee, car lent and accommodation and Katharina Sparre at Helsingborgs stad for car transport making it possible for us to participate in Oresund Electric Car Rally, 12-13 May 2012.

Daniel Andersson and David Carlsson

Göteborg, Sweden, 2012

Contents

Abstract **i**

Acknowledgements **ii**

Contents **iii**

List of figures **iv**

List of tables **1**

1 Introduction **2**
1.1 Previous work 2
1.1.1 Fast charging in Japan 2
1.1.2 Fast charging stations in Sweden 2
1.2 Problem background 3
1.3 Purpose 3

2 Technical background **4**
2.1 Plug-in electric vehicle (PEV) 4
2.1.1 Citroën C-Zero 4
2.1.2 Controller Area Network (CAN) 5
2.2 Lithium-ion battery 6
2.2.1 Battery state of charge 6
2.2.2 Battery of Citroën C-Zero 6
2.3 Charging method 6
2.4 Charge schemes for electric vehicles 7
2.4.1 AC charging 7
2.4.2 DC charging 8
2.5 General design of a fast charging station 9
2.6 Power quality 10
2.6.1 Surrounding grid 10
2.6.2 Voltage levels 11
2.6.3 Harmonics 11

3 Case setup **12**
3.1 Design of ABB PCS DCFC Fast Charger 12
3.2 Yokogawa WT1800 Precision power analyser 15
3.2.1 Connection 15
3.2.2 Preferences 15
3.2.3 Test of the power analyser 16
3.2.4 Current probes 16
3.2.5 Measurement uncertainty 16
3.3 CAN-bus recording 17
3.3.1 Finding CAN connections in the vehicle 17

3.3.2 Vehicle CAN . . . 17
3.3.3 Battery CAN . . . 19
3.3.4 Charging CAN . . . 19
3.4 Collected data . . . 20
3.5 Data analysis . . . 20

4 Results **24**
4.1 Measurements . . . 24
4.1.1 Measurement 1: warm battery pack . . . 24
4.1.2 Measurement 2: warm battery pack . . . 33
4.1.3 Measurement 3: cold battery pack . . . 33
4.1.4 Measurement 4: cold battery pack . . . 34
4.1.5 Measurement 5: half discharged battery . . . 34
4.1.6 Measurement 6: half discharged battery . . . 35
4.1.7 Measurement 7: AC charging with 10 A . . . 35
4.2 Charging behavior . . . 35
4.2.1 Voltage and current characteristic of charging . . . 35
4.2.2 Battery resistance . . . 36
4.2.3 Temperature dependence . . . 37
4.2.4 Charger efficiency . . . 37
4.2.5 Charger and battery efficiency . . . 39
4.2.6 CAN verses power analyser . . . 39
4.3 Power quality . . . 39
4.3.1 Harmonics . . . 39
4.3.2 Voltage dip . . . 46
4.3.3 Reactive power . . . 46

5 Conclusions **50**
5.1 Future work . . . 50

A Appendix **54**
A.1 Matlab code for importing data . . . 54
A.1.1 Importing Yokogawa measurement file . . . 54
A.1.2 Importing CAN data file . . . 55
A.2 Matlab code for scaling and viewing measurement . . . 56
A.2.1 Main program . . . 56
A.2.2 Combine files (createElcCarBatCha.m) . . . 56
A.2.3 Assign and scale data (nameAndScaleData.m) . . . 59
A.2.4 Assign and scale battery CAN data (nameAndScaleBat.m) . . . 64
A.2.5 Plot data (plotAll.m) . . . 65

List of Figures

2.1.1 Citroën C-Zero 4
2.1.2 Example of CAN messages 5
2.2.1 Battery pack of Citroen C-Zero 7
2.2.2 Simple equivalent circuit of a battery 7
2.4.1 CHAdeMO connector to the left and Combo connector to the right 8
2.5.1 Circuit of a fast charger with a line transformer, lower schematic is the DC/DC converter 9
2.5.2 Circuit of a fast charger with a medium frequency transformer, lower schematic is the DC/DC converter 10
2.6.1 Electric grid equivalent 11
3.0.1 General measurement setup 12
3.0.2 Detailed measurement setup 13
3.0.3 Connection of the power analyzer to the ABB fast charger. 14
3.3.1 Connection of Kvaser memorator to battery and vehicle computers. 18
3.5.1 Example of data collected from Car CAN 22
4.1.1 Measurement 1: Voltages, currents, powers and state of charge 25
4.1.2 Measurement 2: Voltages, currents, powers and state of charge 26
4.1.3 Measurement 3: Voltages, currents, powers and state of charge 27
4.1.4 Measurement 4: Voltages, currents, powers and state of charge 28
4.1.5 Measurement 5: Voltages, currents, powers and state of charge 29
4.1.6 Measurement 6: Voltages, currents, powers and state of charge 30
4.1.7 Measurement on AC charging: Voltages, currents, powers and state of charge . 31
4.1.8 Battery and ambient temperature for measurements 1-6 32
4.2.1 DC voltage and current as a function of battery state of charge 36
4.2.2 Charger power output and efficiency as function of state of charge 38
4.2.3 Converter and battery efficiency as a function of DC power 40
4.2.4 Absolute power losses in charger and battery 41
4.3.1 Average harmonics for n=0 to 100 in phase 1 for measurement 2 42
4.3.2 Average harmonics for n=0 to 20 in phase 1 for measurement 2 43
4.3.3 Time dependence harmonics for phase 1 for measurement 2 44
4.3.4 Time dependence harmonics for phase 1 for measurement 3 45
4.3.5 AC phase voltage as a function of phase current 47
4.3.6 Active and reactive power consumed by the charger 48

List of Tables

3.1.1 Specification of ABB PCS DCFC Fast Charger 15
3.2.1 Measurement uncertainty of Yokogawa WT1800 Precision power analyser . . . 16
3.2.2 Measurement uncertainty for harmonics of Yokogawa WT1800 Precision power analyser 16
3.2.3 Measurement uncertainty for the current probe Fluke 80i-500s 17
3.2.4 Measurement uncertainty for the current probe LEM PR2000 17
4.1.1 Measurements performed on ABB prototype fast charger 24
4.2.1 Approximate temperature dependence of charging current 37

1 Introduction

After the economic crisis in 2008 the automotive industry started to develop electric vehicles on a larger scale. Driving forces has been to reduce CO_2 emissions and government funding. The battery technology has also developed a lot, which is necessary in order to reduce price and increase performance of the electric vehicles.

Fast Charging is considered, as one of the key factors in order to have a large fleet of electric vehicles and make it possible to drive longer distances without spending several hours charging the battery and remove range anxiety[10]. With fast charging the charging time is reduced from several hours to 15-30 minutes depending on the charging technique and battery chemistry and temperature..

1.1 Previous work

There has been a lot of studies performed on simulating how fast charging either affects the electric grid or the battery. Many of the studies regarding electric grid consider only rated power of the charger but the rated power is only consumed for the first couple of minutes of the charging, then the power is ramped down in order to not having to high voltage over the battery cells[9].

Today most fast charging stations uses a standard named CHAdeMO , which specification is confidential and not explained in a detail manner in any IEEE paper. The documents that are available mainly comes from Japan where Tokyo Electric Power Company (TEPCO) has been involved in the development of CHAdeMO.

1.1.1 Fast charging in Japan

The number of installed fast charging stations which support CHAdeMO increase fast[5]. In the beginning of 2011 the amount of fast charging station was around 300, but today the number is significant higher, namely 1236. This numbers are only for the Japanese market, to compare with the market in Europe where the total amount of installed fast charging station are 207 in June 2012[5].

1.1.2 Fast charging stations in Sweden

For the moment, there are six fast charging stations installed in Sweden, which uses CHAdeMO. Three of them are prototypes, installed for testing and evaluation[8].

In Göteborg, the organisation Test Site Sweden (TSS) has a goal to support sustainable transportation. TSS provides test environments for vehicle technology and surrounding infrastructure. One of the projects, which was started in the summer 2011, is to set up two CHAdeMO fast charging stations in Göteborg. The funder of the project is Region Västra Götaland, their partner Göteborg Energi is responsible for installation of the fast charging stations, ABB and Turning Point are responsible for supplying the chargers. One of the fast charging stations is installed at Gatubolaget, who have three electric converted Fiat and one at H-O Enterprise who toady have three cars with support for CHAdeMO.

The municipality of Östersund, Sundsvall, Trondheim and their electricity dealers takes part in a project, Green Highway, with goal of having a fleet of 15% electric vehicles in 2020 compared to a few hundred in Sweden today. One part of the project is to make it possible to drive from Sundsvall to Trondheim with an electric vehicle without spending several hours charging the car. As a pre-study an ABB fast charging stations has been installed in Östersund[1].

In Stockholm there are currently two fast charging stations provided by the car dealer Mobility Motors, one in Sätra and one in Bromma. The fast charging stations were installed this spring when they started to sell the electric vehicle Nissan Leaf[7].

Also in Malmö, Mobility Motors installed one fast charging station to provide the customer with the possibility of fast charging[8][5].

1.2 Problem background

This master thesis is performed at HRM Engineering, a consultant company in Göteborg. They have long experience from the auto industry and have been involved in many projects regarding electric vehicles, mainly for Volvo cars and the Norwegian electric car THINK City. One of their strategic goals is to take step towards infrastructure projects related to charging of electric vehicles. This master thesis is a first step and will focus on evaluating a prototype station for fast charging, ABB PCS DCFC fast charger, in Göteborg.

1.3 Purpose

The purpose of this study is to evaluate a prototype fast charger from ABB, PCS DCFC fast charger, which is installed in Göteborg. With a whole concept focus, also the grid influences from the fast charging station such as voltage dips and harmonics together with the electric vehicle battery pack was considered. Charging performance, such as efficiency with different conditions on the battery SOC, internal battery temperature and ambient temperature will be analysed. Regarding the efficiency, a comparison between fast charging and normal charging with AC will be performed.

2 Technical background

This chapter present a technical overview of the used vehicle Citroën C-Zero, different charging strategies and electrical components of ABB prototype fast charging station. Also, the setup of the measurements are described and discussed.

2.1 Plug-in electric vehicle (PEV)

Plug-in electric vehicle (PEV) is a subcategory of electric vehicle (EV). The PEV has battery that can be recharge from the electric grid[16]. There are two types of PEV:s battery electric vehicles (BEV) and plug-in hybrid electric vehicles (PHEV)[17][16]. BEV has no combustion engine and must be charged from the electric grid. PHEV has an electric drive system and a combustion engine that can charge the battery.

2.1.1 Citroën C-Zero

Figure 2.1.1: *Citroën C-Zero*

The first electric vehicle in Sweden with support of fast charging with CHAdeMO, was Mitsubishi i-MiEV and its European sister Citroën C-Zero, Figure 2.1.1, which will be used in this thesis. It has a 47kW (64hp) electrical permanent magnet synchronous motor and accelerates from 0-100km/h in 15s[23]. Citroën claims the range to be 150km and test performed by Gröna Bilister verifies that it is valid for speed at 65km/h and with the air conditioning switch off[25]. More reasonable range at mixed driving is 120-130km[25]. The charging time with 230V one phase AC is 8-9 hours with 10A and 7 hours with 16A. With fast charging at 50kW the charging time is specified to 30 min (fast charging is specified as 0% to 80% state of charge). The power consumption is approximately 1.3kWh/km which corresponds to approximately 1.5SEK/10 km[25]. The battery has warranty for 5 years but no specific data has been found regarding the life time of the battery.

2.1.2 Controller Area Network (CAN)

CAN is a serial bus system which was developed by Bosch and became an automotive standard in 1993 as ISO 11898-1. It is a standardized system used for communication in the vehicles. CAN is a broadcast communication where every module connected to the network can send out messages to all other modules. Every message has a unique identifier and the priority of the messages is set by the message-unique identifier. Lower identifier gives higher priority. The bus does not need to be modified when a new module is connected[27].

Format of the CAN Message

The CAN standard decides how the message is constructed and the important parts of the message are the identifier (ID), data length code (DLC) and data field, see Figure **??**. The identifier is a 11 bit long integer and is an unique identifier for each message. The data length code is a 4 bit integer which states how long the data field is. The data field is the part of the message that contains the information broadcasted. The field is 0-64 bit long which corresponds to 0-8 bytes which is a number between 0 to 255.

In order to transmit data values larger than one byte (255) two or more bytes can be used (two bytes gives numbers between 0 to $2^{16} = 65536$). Data can also be scaled by a factor and offset in order to represent values outside the range 0 to 255.

```
Time            ID                          DLC  Data field (0-8 bytes)
------------------------------------------------------------------------------
380.2420        288                      Rx d 8   07 d0 27 10 ad 00 11 10
380.2430        6d4                      Rx d 8   00 00 00 00 00 00 00 00
380.2440        236                      Rx d 8   10 1c 10 00 a0 00 00 b6
380.2450        418                      Rx d 7   50 00 e2 00 56 00 00
380.2470        212                      Rx d 8   00 00 00 00 a7 d0 00 00
380.2540        236                      Rx d 8   10 1c 10 00 b0 00 00 ae
380.2540        101                      Rx d 1   04
380.2560        346                      Rx d 8   28 ea 51 20 00 00 00 41
380.2570        325                      Rx d 2   01 00
380.2570        424                      Rx d 8   43 00 0c 00 a9 c7 01 ff
380.2570        208                      Rx d 8   00 20 60 00 c0 00 c0 00
```

Figure 2.1.2: *Example of CAN messages*

The manufacture of the vehicle builds a database of what every identifier and byte represents. For example a message with identifier 245 can be sent from the battery management computer and byte 1 be the temperature of the battery with an offset of -40 in order to have temperatures between -40 and 215^{o}C and byte 2 the battery state of charge scaled with 0.5 in order to have values between 0 and 128%. If the CAN database is not known the representation and scaling of the frames can be guessed by comparing the data of each frame with known qualities. An example of a recorded message from the CAN bus is shown in Figure 2.1.2.

2.2 Lithium-ion battery

A battery built up by battery cells connected in series and parallel, each cell has three fundamental components: anode, cathode and electrolyte. The materials for the different components decide characteristics and capacity of the battery.

In a Lithium-ion battery the electrolyte is usually made from different types of lithium salts. The cathode is usually made of lithium cobalt oxide and the anode is usually made of graphite. This materials gives the lithium-ion battery a nominal cell voltage of 3.75V. This gives the lithium-ion battery the advantage of a high energy density[4].

2.2.1 Battery state of charge

Battery state of charge is represented in percent of the battery capacity which is measured in kWh. When the battery age the capacity decreases, so 50% state of charge for a 16kWh battery can in the beginning correspond 8kWh and after some years 6kWh du to aging of the battery[27]. Battery state of charge cannot be measured directly. Instead there are a numerous of techniques for estimation and two common methods which often are combined are voltage method and current integration method[13].

The voltage method relates open circuit voltage to the battery state of charge using a known relationship. The disadvantage with this method is the battery must stabilize when no current is drawn due to the capacitive characteristic. Also, the battery voltage needs to be corrected depending on the battery temperature.

The current integration method calculates the state of charge by integrate the current in and out of the battery. The disadvantage is the lack of reference point which makes the method sensible to long term measurements error.

2.2.2 Battery of Citroën C-Zero

The main battery of C-Zero, Figure 2.2.1, has a capacity of 16kWh (68MJ) and a nominal voltage at 300V. It is built up by 88 lithium-ion cells with a capacity of 50Ah and nominal voltage of 3.75V each. Each cell is designed for voltages between 2.5-4.5V which gives 220-396V for the whole battery pack.

The resistance for a single cell is 1.5mΩ, which give a total internal resistances of 132mΩ and estimation of the ohmic losses in the battery is $P = RI^2$. One of the most simple models of a battery is an ideal battery, with voltage E, in series with a parallel connected resistance R and capacitance C, Figure 2.2.2. The battery is located below the front and back seat and consist of two 4-cells modules and ten 8-cells modules.[27]

2.3 Charging method

A Lithium-ion battery is charged with DC using a method called constant current constant voltage (CC/CV). As the name indicates, the charge process executes in two steps: under the first step the current is constant until the voltage reaches a predefined upper value. At this point, step two begins. The voltage is now constant on the predefined limit, meanwhile the current is ramped down in order to keep the voltage constant. There are two ways to terminate the charging process, either by predefine the time in constant voltage mode, or

Figure 2.2.1: *Battery pack of Citroen C-Zero*

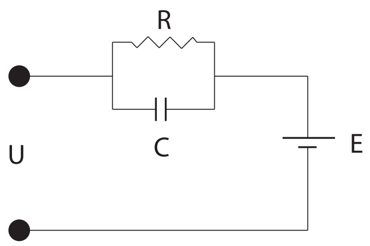

Figure 2.2.2: *Simple equivalent circuit of a battery*

when the charging current in constant voltage mode drops under a certain predefined value. By increasing the charging current in the constant current mode the charging time decreases, but the drawback is ageing and risk of destroying the cells. A compromise between a faster charging and minimize the ageing is a fact. Regarding the ageing aspect on a battery, the importance of not violating the different temperature and potential constrains. For more detail reading about charging strategies and its constrains see reference[9].

2.4 Charge schemes for electric vehicles

Today there are two different techniques for charging electric vehicle: AC charging and DC charging[10].

2.4.1 AC charging

AC charging uses an on-board charger and the vehicle is connected to the AC grid. AC charging is also referred to as normal charging or residential charging and uses one phase[15]. In Sweden one phase 230V with fuses at 10 or 16A are used, which give powers of approximately 2 or 3.7kW. For a battery of 16kWh with 20% state of charge, the charging time is between five to eight hours.

2.4.2 DC charging

DC charging uses an external charger i.e. that the vehicle is fed by DC current directly to the battery. DC charging is also referred to as fast charging, rapid charging and quick charging. In the future solutions for ultra-fast charging up to 250kW could be available which gives a charging time of some minutes for a 16kWh battery. Today, the maximum power is limited to 50kW because when battery exposes for to high current or to high cell voltages the battery life time decreases. Charging time is approximately 30 minutes for charging a 16kWh battery to 80%[10]. The charger must be able to adapt its output to 100-500V in order to meet different voltage levels on different car battery packs[3].

The heat generation is a major issue so the charging process must be controlled and limited if necessary. Some car models for example Citroën C-Zero have an active cooling which activates when the temperature exceeds a certain limit.

CHAdeMO standard

The most commonly used standard for fast charging today is CHAdeMO, which is an outcome from a collaboration between Japanese auto makers (Fuji Heavy Industries, Mitsubishi, Nissan and Toyota) and Tokyo electric power company (TEPCO). The standard supports up to 50kW DC charging at voltages between 100-500V[14]. The larger number of EV with support for CHAdeMO in Japan and EU has led to an increased number of charging stations and CHAdeMO is today de facto industry standard[12]. The connector for CHAdeMO can be seen in Figure 2.4.1.

Figure 2.4.1: *CHAdeMO connector to the left and Combo connector to the right*

One drawback with CHAdeMO is that the vehicle needs two charging connectors, one for AC and one for DC charging. This makes the design of the vehicle less clean, more expensive and the driver must know which charging connector to use. Another disadvantage is the limited power of 50kW. Today most battery can only handle 50kW but in the future higher power rate will probably be demanded[3].

Competing standards

In a new standard called Combo from Society of Automotive Engineers, SAE, both AC and DC charging is combined in a single connector. The connector supports one and three phase AC charging and DC charging. The AC connector is the same as being used by most cars today. The DC connector supports 200A or 100kW at 500V which is double as high compared to CHAdeMO.

So far, three American (Chrysler, Ford and General Motors) and five German (Audi, BMW, Daimler, Porsche and Volkswagen) auto makers have decided to use the Combo which is planned to be introduced to the market in 2013[6].

2.5 General design of a fast charging station

The power electronics (PE) in a fast charging station basically consist of a transformer, AC/DC converter and a DC/DC converter. The type of PE can be varied in different fast charging stations. Basic requirement from the safety standard, is to have a galvanic insulation between the power grid and the battery pack. This can be achieved in two ways, either with a low frequency (LF) or a high frequency (HF) concept. Both the concepts must ensure that the charging process is fully safe, secure and have a high efficiency.

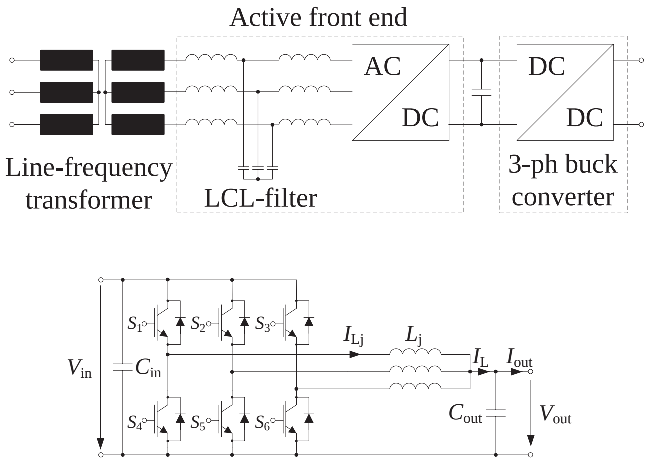

Figure 2.5.1: *Circuit of a fast charger with a line transformer, lower schematic is the DC/DC converter*

The LF concept uses a 1:1 turns ratio line-frequency transformer connected to the grid, to obtain a galvanic insulation. To fulfill the international IEC harmonic injection standard a LCL filter is installed after the transformer. To ensure an active power factor control on the line side, a three phase active rectifier unit is installed. The rectifier also provides an interleaved buck converter with a constant DC-link with a voltage of 750V. The three phase interleaved buck converter consist of six insulated gate bipolar transistors (IGBT) and three inductors. It has been proofed that, to meet the best output current profile a switching frequency of 2kHz is preferable[3]. Furthermore inductors are connected in a star point connection on the secondary side. This means that the output power can be distributed over three different converter branches, which in turn reduces the stress and the losses for the whole converter. The LF concept support vehicle to grid operation.

For the HF concept the line-frequency transformer is not needed, instead the LCL filter with the same purpose as before is connected to the power grid. With the same requirements as for the LF concept also a three phase active rectifier unit is installed. To fulfill the safety standard two in parallel DC/DC isolated converter are implemented. To be able to adjust the

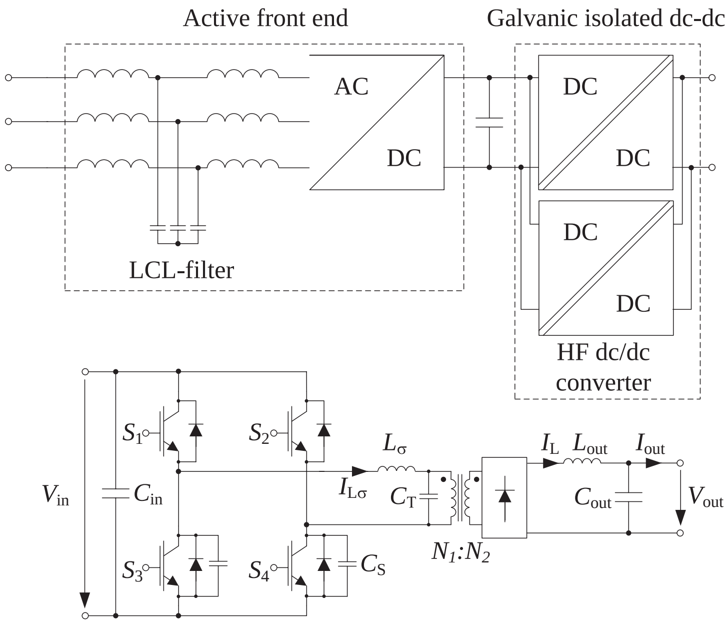

Figure 2.5.2: *Circuit of a fast charger with a medium frequency transformer, lower schematic is the DC/DC converter*

output voltage applied on the battery, the DC/DC converters contain a single phase inverter. The inverter is fixed to operate at a constant frequency at 8kHz. The galvanic isolation obtains from a medium frequency transformer, which is installed between the inverter and the rectifier. By implement some active components to the rectifier, the HF concept can also be used for output power from the vehicle to the electric grid[3].

2.6 Power quality

The Swedish guideline for power quality in the low voltage grid can be found in standard SS-EN 61000-2-2[20]. The standard covers low voltage part of the grid with voltage levels of maximum 420V one phase and 690V three phase with 50 or 60Hz as nominal frequency.

There are several types phenomena affecting the power quality: In this thesis focus will be on voltage dips and asymmetries, voltage and current harmonics, flicker and transients[18].

2.6.1 Surrounding grid

The electric grid surrounding the fast charger can from the fast charger perspective be represented by a voltage source U_{grid} in series by a complex impedance Z_{grid} see Figure 2.6.1. The values of U_{grid} and Z_{grid} varies depending on other loads in the electric grid, position of tap changers etc. This implies that the voltage at the connection point of the fast charger varies over time. If the grid is weak, which is common when the connection point is far away from closest substation, other loads can decrease the voltage because of the voltage drop in the lines becomes higher because of the higher current.

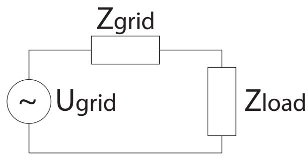

Figure 2.6.1: *Electric grid equivalent*

2.6.2 Voltage levels

The voltage in the grid varies depending on the load and distance to the grid station. The highest voltage level is found close to the grid station and is lowerd far out in the grid. Many electrical devices are constructed for voltage within a certain range, for example ABB's new fast charging station Terra 51 specifies a working voltage at $400 \pm 10\%$[2].

2.6.3 Harmonics

Harmonics can appear both in currents and voltages and are integer multiples of the grid frequency (50Hz). In the Swedish electric grid there are almost only odd multiples. The harmonics are usually refer to as percent of its fundamental

$$\frac{U_n}{U_1} 100\% \tag{2.6.1}$$

$$\frac{I_n}{I_1} 100\% \tag{2.6.2}$$

where n represents the harmonics multiple U_n and I_n of the fundamental U_1 and I_1[19].

Total demand distortion

Normally the total harmonics is presented by total harmonics distortion, (THD) where the square root of sum of all harmonics in square is divided by the fundamental as

$$THD = \sqrt{\sum_{2}^{\infty} \left(\frac{U_n}{U_1}\right)^2} 100\% \tag{2.6.3}$$

For the voltage, which has a nominal value of 400V, this can be easily compared. But for the current which varies, a better way of presenting the THD is to use Total Demand Distortion TDD

$$TDD = \sqrt{\sum_{2}^{\infty} \left(\frac{I_n}{I_{ref}}\right)^2} \cdot 100\% \tag{2.6.4}$$

where the fundamentals current I_1 in the denominator is changed to the nominal current I_{ref}. The same can be performed for the voltage[19] as

$$TDD = \sqrt{\sum_{2}^{\infty} \left(\frac{U_n}{U_{ref}}\right)^2} 100\% \tag{2.6.5}$$

3 Case setup

This chapter describes the measurement setup and the measurement equipment used in this study. The fast charger station which is analysed and evaluated is ABB PCS100 DCFC DC Fast Charger, which is a prototype and will not be introduced to the market. The specification of the charger can be found in Table 3.1.1. The fast charging station is installed at H-O Enterprise in Agnesberg which is located in the north of Göteborg.

Figure 3.0.1 gives an overview of the system and how the measurement equipment are installed. The DC current is feed through the charging pole to the battery in the vehicle.

The voltages are measured on all three AC phases and on the DC side between the converter and the charging pole, this is done with a power analyser, see Figure 3.0.3. The current is measured at the same point by current clamps in order to avoid modifying the existing connection. To ensure a safe voltage measurement insulated cables with built in fuses are used for voltage measurements. Figure 3.0.2 gives a more detailed schematics of the measurement setup.

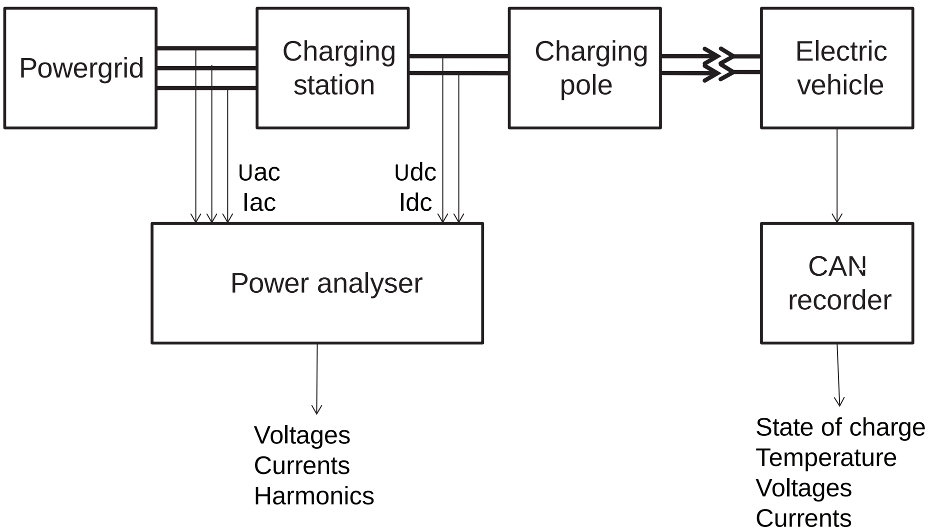

Figure 3.0.1: *General measurement setup*

3.1 Design of ABB PCS DCFC Fast Charger

The fast charging station used in this study is a prototype development by ABB. The power electronic architecture is similar to the LF concept, described in previous section. The input power is rated to 80kVA with a power factor of 0.95. Output voltage is in the range of 50-550V DC and the recommended temperature is between 0-40°C. The data sheet for the fast charging station is provided in Table 3.1.1

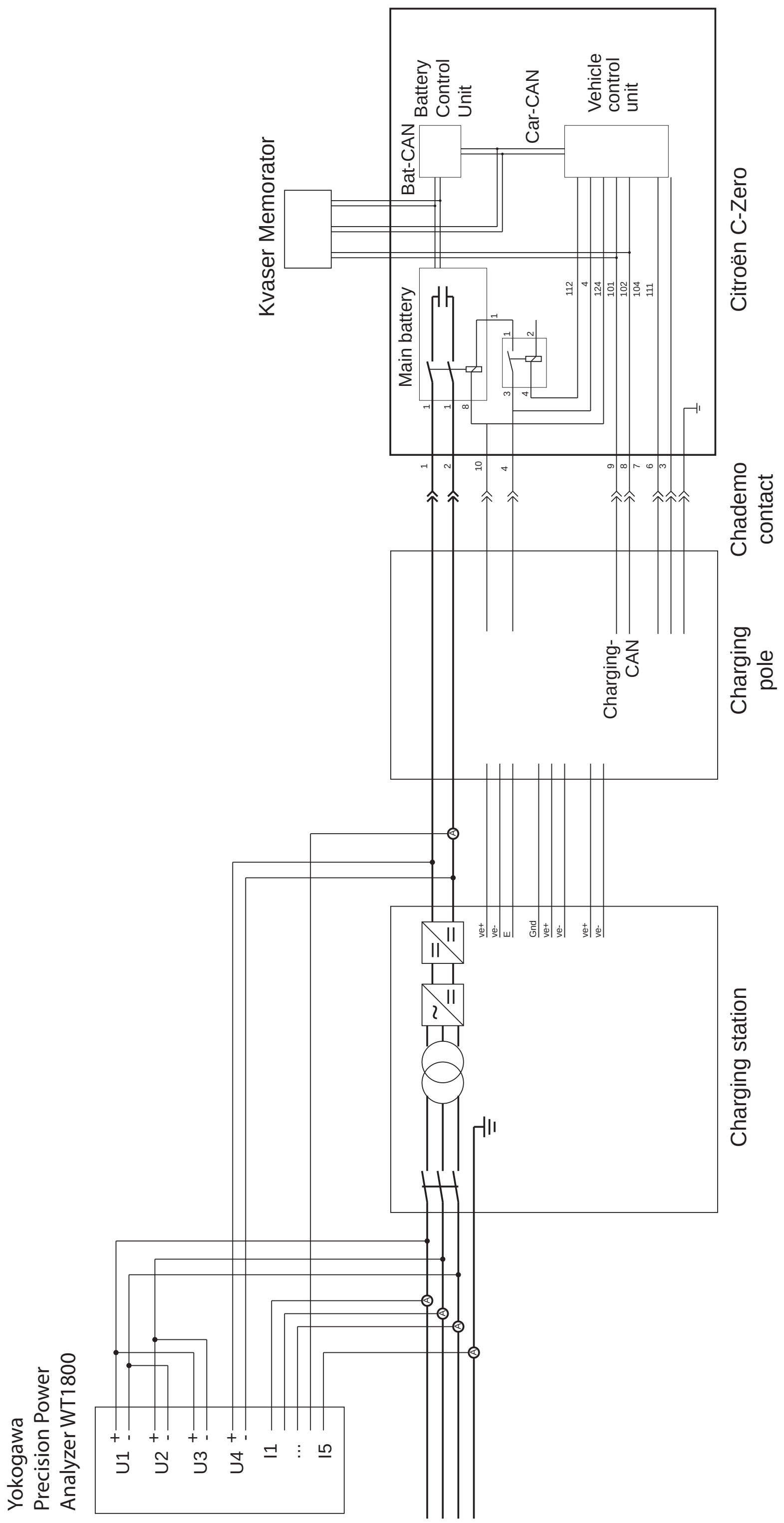

Figure 3.0.2: *Detailed measurement setup*

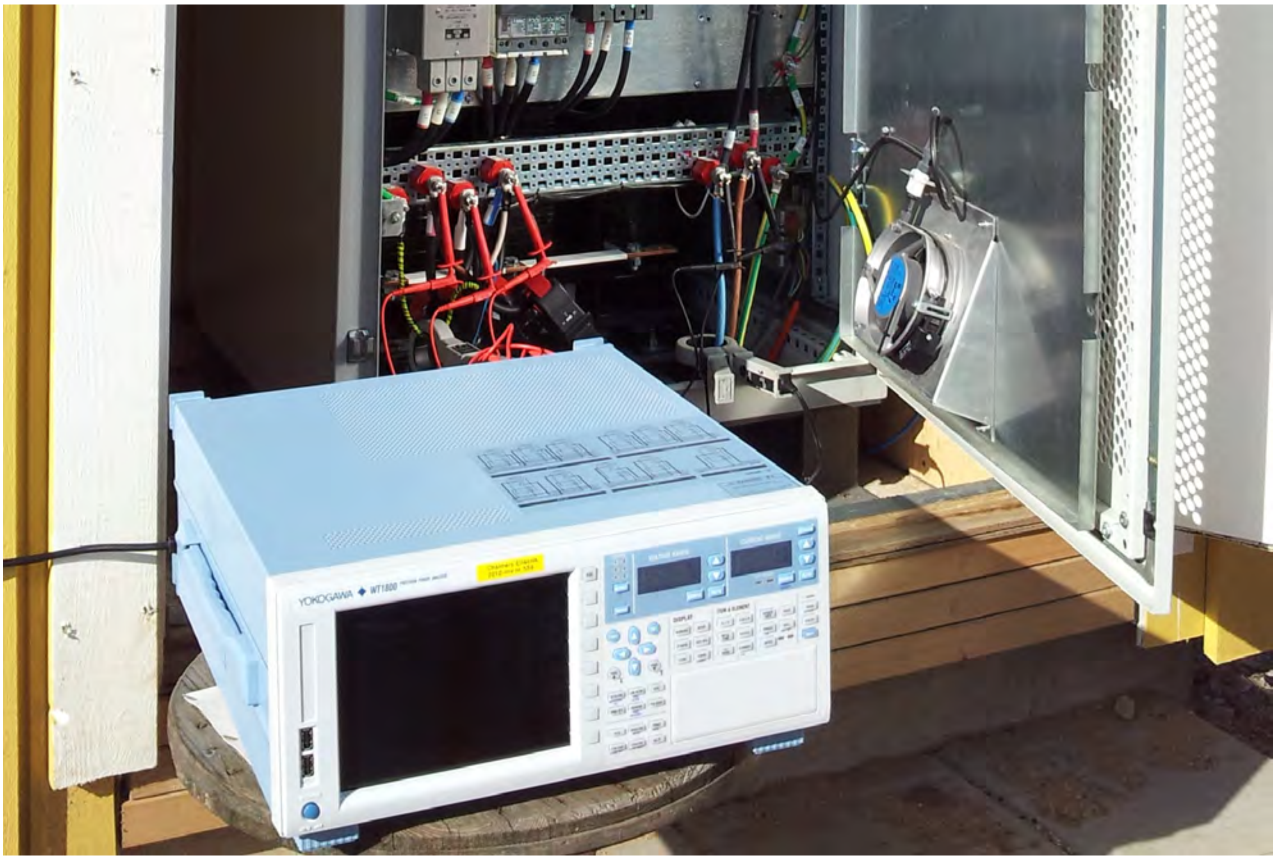

Figure 3.0.3: *Connection of the power analyzer to the ABB fast charger.*

Table 3.1.1: Specification of ABB PCS DCFC Fast Charger

Input	
Voltage	380/400Vac 3Ø, 50/60Hz
Power	80kVA >0.95pf
Current	120A
Earthing System	TN-S Star Point Earthed
Installation Category	III
Output	
Voltage	50-550Vdc
Current	0-125Adc
Earthing system	IT
Environmental	
Temperature	0-40^{o}C Recommended
IP Rating	Converter IP20 / Pole IP44
Pollution Degree	2

3.2 Yokogawa WT1800 Precision power analyser

In order to measure voltage and current on both AC- and DC-side simultaneously a Yokogawa WT1800 Precision power analyser is used. It has six channel input with separated voltage and current input for each channel. This makes it possible to measure all three AC phases and DC simultaneously.

3.2.1 Connection

Since there is no neutral point available as a reference, the wiring system is selected in order to use the main voltages, see Figure 3.0.3 for a picture of the setup. The wiring setup can be found in Figure 3.0.2. The maximum current the power analyser can measure is 50A, which is not enough so current clamps is used. By using current clamps the connection of the charging station does not need to be modified or disconnected from the grid when the measurement equipment is connected. The voltage clamps are attached directly on the bolts where the conductors are connected.

3.2.2 Preferences

The Yokogawa sampling rate is 2MHz but it does not store collected data with this rate. Instead it performs calculations every 50ms to 20s and store the calculated data. The record rate is selected to 50ms in order to get as high resolution as possible. The calculated quantities are RMS values of voltage, current, active, reactive and apparent power. The power is also integrated in order to measure how much energy that is consumed and transfers to the vehicle by the charging station. Also voltage and current RMS harmonics up to 5kHz is recorded every 50ms in order to analyse power quality and its effects on the grid.

3.2.3 Test of the power analyser

The power analyser contains many useful functions, but in order to be able to sort and apply them for measuring fast charging, testing has been performed in a laboratory at Chalmers. To achieve a realistic model for fast charging measurement the test model must contain both DC and AC. This is done by using the DC-machine and the induction machine in the laboratory. Different connection schemes are available for the power analyser, but the measurements on the fast charging station limits the options to one, due to no neutral point. So measurements are performed with the 3P3W scheme and are referred to [11].

3.2.4 Current probes

For the DC side the current clamps LEM PR2000 are used. Because of limit amount of LEM PR2000 current probes another type has been used for current measurements on AC-side, namely the Fluke 80i-500s current probe.

3.2.5 Measurement uncertainty

The power analyser's accuracy for the voltage, current and power is presented in the Table 3.2.1. Furthermore, the accuracy for harmonic measurement is presented in Table 3.2.2.

Table 3.2.1: Measurement uncertainty of Yokogawa WT1800 Precision power analyser

Measured unit	Frequency	Accuracy ±(reading error + measurement range error)
Voltage	DC	±(0.05% of reading + 0.1% of range)
	45-66Hz	±(0.1% of reading + 0.05% of range)
Current	DC	±(0.05% of reading + 0.1% of range)
	45-66Hz	±(0.1% of reading + 0.05% of range)
Power	DC	±(0.05% of reading + 0.1% of range)
	45-66Hz	±(0.1% of reading + 0.05% of range)

Table 3.2.2: Measurement uncertainty for harmonics of Yokogawa WT1800 Precision power analyser

Frequency	Voltage	Current	Power
45-66Hz	0.05% of reading + 0.25% of range	±(0.05% of reading + 0.1% of reading) + 0.25% of range	 + 0.5% of range

The accuracy for the power analyser is depending on both humidity and temperature, where the temperature should be between 18-28^{o}C and the relative humidity between 30% to 75%, for the specifications in Table 3.2.1 and 3.2.2 [11]. When using external current sensors an uncertainty factor of 50μV must be added to the values in the Table 3.2.1.

The measurement accuracy for the current probe Fluke 80i-500s is presented in the Table 3.2.3 and for LEM Pr2000 it is presented in the Table 3.2.4.

For the current probe Fluke 80i-500s, the temperature also influence on the accuracy. Between -10 to 18^{o}C and for the interval 28 to 50^{o}C, an additional percent of <0.15% per 10^{o}C

Table 3.2.3: Measurement uncertainty for the current probe Fluke 80i-500s

Frequency	Current range	Error	Phase shift
45-66Hz	1 to 20 A	5% of reading + 0.3 A	Not specified
	20 to 100 A	5 % of reading	±3 degrees

must be added to the uncertainty[24]. The output rate is 1mV/1A.

Table 3.2.4: Measurement uncertainty for the current probe LEM PR2000

Frequency	Current range	Error
DC to 10kHz	2000 A	± 1% of reading ± 500 mA

The current probe LEM PR 2000 has the accuracy according to Table 3.2.4 at a temperature of 25^{o}C. But when the temperature differs a temperature coefficient of $\pm 0.1\%/1^oC$ must be added [26]. The output rate is 1mV/1A.

The measurement uncertainty for the power analyser with current clamps is very slight, one example is presented with values from measurement one. For the AC voltage a maximum uncertainty is ±0.7V and for the DC voltage it is ±0.78V. The AC current has a maximum uncertainty of ±3.5A and the DC current ±1.55A. The total uncertainty is so small that there is no qualitative influence on the measurement result. Since the measurements is performed outdoor influences from humidity and varying temperatures is a fact, but because of the difficult possibilities to control this quantities no major consideration is done.

3.3 CAN-bus recording

Citroën C-Zero has three CAN-buses. One is the vehicle CAN where most of the computers in the vehicle communicate. The battery also has an own CAN bus where the different cells in the battery transmits its temperatures and cell voltages to the battery management system (BMS). The last CAN-bus is the charging CAN which goes from the main computer to the CHAdeMO connector and in which communication to the fast charging station is performed. The CAN communication is recorded using two CAN-loggers which have two channel each. One channel is used to record the data on the vehicle CAN-bus, one to record the battery CAN and one for the charging CAN. The connection to battery and charging CAN can be seen in Figure 3.3.1.[27]

3.3.1 Finding CAN connections in the vehicle

To be able to record the CAN signals in the vehicle the CAN-buses must be located. A data sheet is used to locate the specific CAN-buses. Since a lot of important data is transmitted on the CAN-bus the sniffing method is used. This method makes is possible to record the available data without interrupting the communication.

3.3.2 Vehicle CAN

The CAN logger is connected to the service port at the driver seat. The communication is recorded using Kvaser memorator professional HS/HS. The goal is to find data related to the

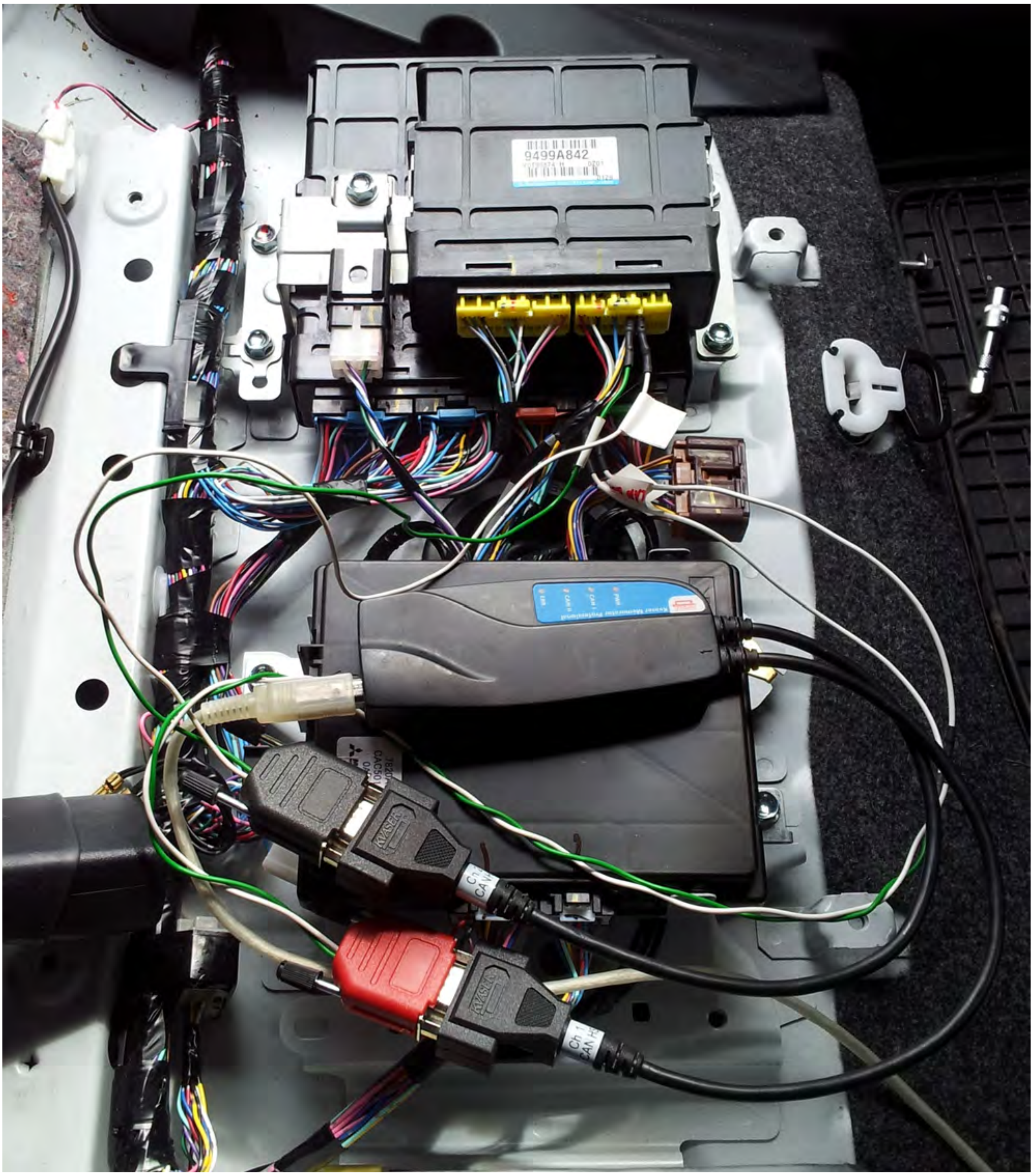

Figure 3.3.1: *Connection of Kvaser memorator to battery and vehicle computers.*

charging such as:

- Battery state of charge
- Main battery voltage
- Charging current
- Battery temperature
- Ambient temperature

The data from the CAN bus can be verified with the quantities measured with the power analyzer and a thermometer. The battery temperature can be compared with those found on battery CAN which has less different quantities than the main vehicle CAN.

This CAN bus is the hardest to find all required quantities on because there is a lot of different data transmitted. When the vehicle is charging only some of the ID:s are active and a lot of the data is zero, which makes it easier to find the desired values.

3.3.3 Battery CAN

The CAN logger is connected to the battery management system located under the back seat and the data is recorded using Kvaser USBScan2 (HS/HS) channel 1. The connection can be seen in Figure 3.3.1. The battery CAN bus should contain the following quantities from each of the eight cell packs:

- Cell voltages
- Cell temperatures

The ID:s were numbered in a way so it was quite easy to find which CAN ID:s sent from the same cell pack. Also the quantities in the message was quite easy to scale and relate to the right quantity by knowing the nominal cell voltage should be 3.75 V and the normal operating temperature of the battery is 30-40^{o}C. The recordings from the battery CAN will only be used to find the corresponding values on the vehicle CAN and no results are presented in this thesis.

3.3.4 Charging CAN

The CAN logger is connected to the vehicle main computer located under the back seat and the data is recorded using Kvaser USBScan2 (HS/HS) on channel 2. The CHAdeMO interface uses both digital and analog communication and the thesis only focuses on the digital CAN communication. The data which is expected to be found on the CAN bus are:

- Battery voltage
- Requested current
- Battery state of charge

There should be a limited number of ID:s on the charging CAN because the communication is only between the vehicle main computer and the fast charging station. The quantities that are of interest can easily be verified with the quantities measured by the power analyzer.

3.4 Collected data

In order to evaluate the fast charging station, voltages and currents are measured on both the AC and DC side of the charger. From there, power, energy, harmonics and efficiency is calculated by the power analyzer and sampled every 50ms.

The active power is calculated using

$$P = UI \cos \Phi \tag{3.4.1}$$

where Φ is the phase angle and the reactive power is calculated from

$$Q = UI \sin \Phi \tag{3.4.2}$$

The power analyzer has a function to integrate power to get energy

$$E = \int_0^t P dt \tag{3.4.3}$$

and an user defined function to calculate the efficiency for the charger

$$\eta = \frac{P_{dc}}{P_{ac}} \tag{3.4.4}$$

where P_{dc} is the power fed to the car and P_{ac} is the power from the grid.

On the vehicle side the voltage, current, temperature and state of charge are recorded from the CAN-bus. The sampling time depends on how often the data is transmitted to the CAN-bus. In order to compare this quantities with the data from power analyser the same calculations is done numerical in Matlab, for calculations refer to appendix A. Because of the different interval of the data transmission the average value has been calculated for every 0.05 to 1s depending on the sampling rate.

The battery state of charge in the CAN bus have been calculated to kWh in order to be comparable with the measurements from the power analyzer. The formula used is

$$E_{power\,analyzer} = E_{CAN}/100 * 16000 \tag{3.4.5}$$

where $E_{power\,analyzer}$ is the power measured by the power analyzer, E_{CAN} is the battery state of charge in percent, the division by 100 is the percent representation in the CAN data and 16000 is the capacity in Wh of the battery pack.

3.5 Data analysis

The collected data from the power analyzer and Kvasers memorator was imported into Matlab. The data was then synchronised with respect to time, by plotting the voltages and currents on the same plot and adding a time offset to the power analyzer measurements. When the CAN signal for battery state of charge was found an offset representing the remaining energy in the battery was added to the integrated energy from the power analyzer.

The CAN-data was plotted as in Figure 3.5.1 for all ID:s and from the plots the interesting quantities were found. For example by looking at frame 5 and 6 in Figure 3.5.1 it can be seen that when the plot in frame 6 becomes zero, it then continues at 255 and at the same time the data in frame 5 increases one step. By combining the data from frame 5 and 6 and then comparing it with the data collected with the power analyzer, it can be seen that the combined plot from frame 5 and 6 is similar to the DC voltage. By scaling the CAN value as

$$(255 \cdot ID883(:,3) + ID883(:,4))0.1 \tag{3.5.1}$$

it becomes very similar to the value from the power analyzer. By the same principle the currents and state of charge were found. The temperature was found by comparing CAN-values with readings from a thermometer. All temperatures were offset from the raw CAN value with -40 and by that the battery, ambient and cabin temperatures were found.

When the slow charge was performed the CAN data had to be time synchronised with the power analyzer. One ID gave its values every 10ms and another every 100ms. The sampling rate from the power analyzer was set to 500ms in order not to handle to large data file. The CAN data was time synchronized to the measurements from the power analyzer in Matlab.

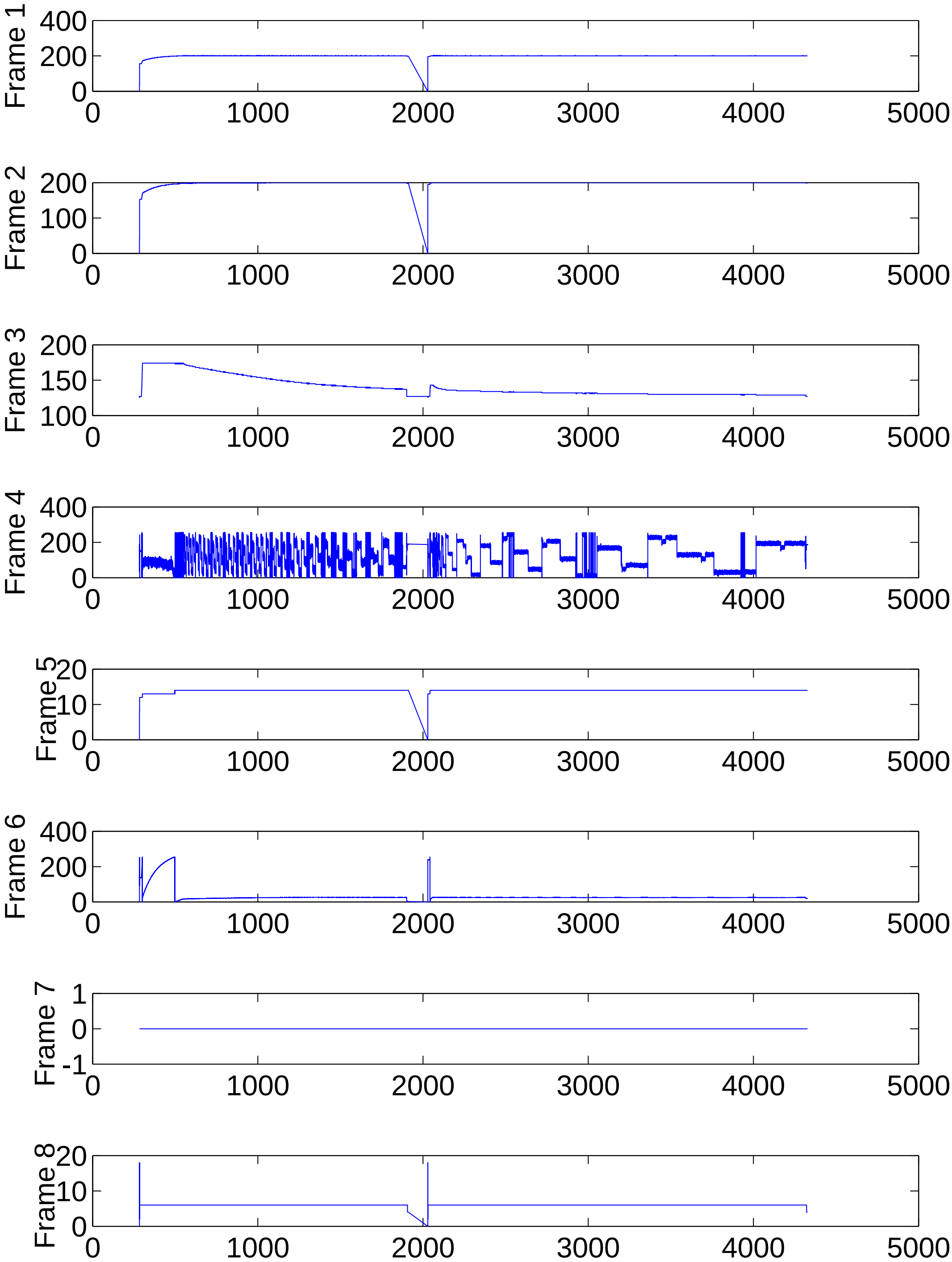

Figure 3.5.1: *Example of data collected from Car CAN*

4 Results

The first part of this chapter describes the different measurements and presents the voltage, current, temperatures and battery state of charge recorded by the power analyzer and CAN. The second part compares the cases with respect to initial state of charge, ambient temperature and battery temperature. In the last part the impact on grid and power quality are discussed.

4.1 Measurements

Six different measurements were performed on the ABB prototype fast charger with different battery state of charge, ambient temperature and battery temperature, see Table 4.1.1. In Figure 4.1.1 to 4.1.6 the measurement data are presented. Voltages and currents are visualized in four different graphs. To the left are the AC voltages and currents of the fast charger with U1 to U3 as the three main voltages and I1 to I3 as phase currents. To the right are the voltage and current on the DC side with Udc and Idc measured by the power analyzer and the others recorded from the CAN data. At the bottom left the AC and DC powers is plotted. Pac and Pdc is measured with the power analyzer, Car CAN Udc*Idc is calculated as Car CAN Udc multiplied by Car CAN Idc and Car CAN d/dt(SOC) is calculated as the numeric derivative of Car CAN SOC. To the bottom right the battery state of charge and in- and output energy of the fast charger. The ambient and battery max/min temperature collected by the CAN data is to be found in Figure 4.1.8 for all six measurements.

A normal charge with 10A AC was also performed. Figure 4.1.7 shows the same data for the slow charge, the difference from previous measurements is that only one phase is used, represented by Uac and Iac and the DC voltage and current were not measured by the power analyzer.

Table 4.1.1: Measurements performed on ABB prototype fast charger

Measure-ment	Date	Initial SOC %	Initial min / max battery temperature ^oC	Initial ambient temperature ^oC	Charging time to approx. 80% SOC min
1	2012-03-21	17.5	27 / 30	19	23
2	2012-04-02	10.0	22 / 27	18	25
3	2012-04-03	10.0	07 / 14	-4	62
4	2012-04-05	9.5	10 / 15	-1	55
5	2012-05-04	43.5	24 / 26	23	21
6	2012-04-27	50.0	31 / 32	26	17

4.1.1 Measurement 1: warm battery pack

The first measurement is performed on a warm battery pack. The trip mileage counter displayed 7km until the battery is empty (normal range for a C-Zero is 100-150km).

In Figure 4.1.1 the voltages, currents, powers and battery state of charges are plotted from the measurements with the power analyzer and CAN data. The ambient and battery

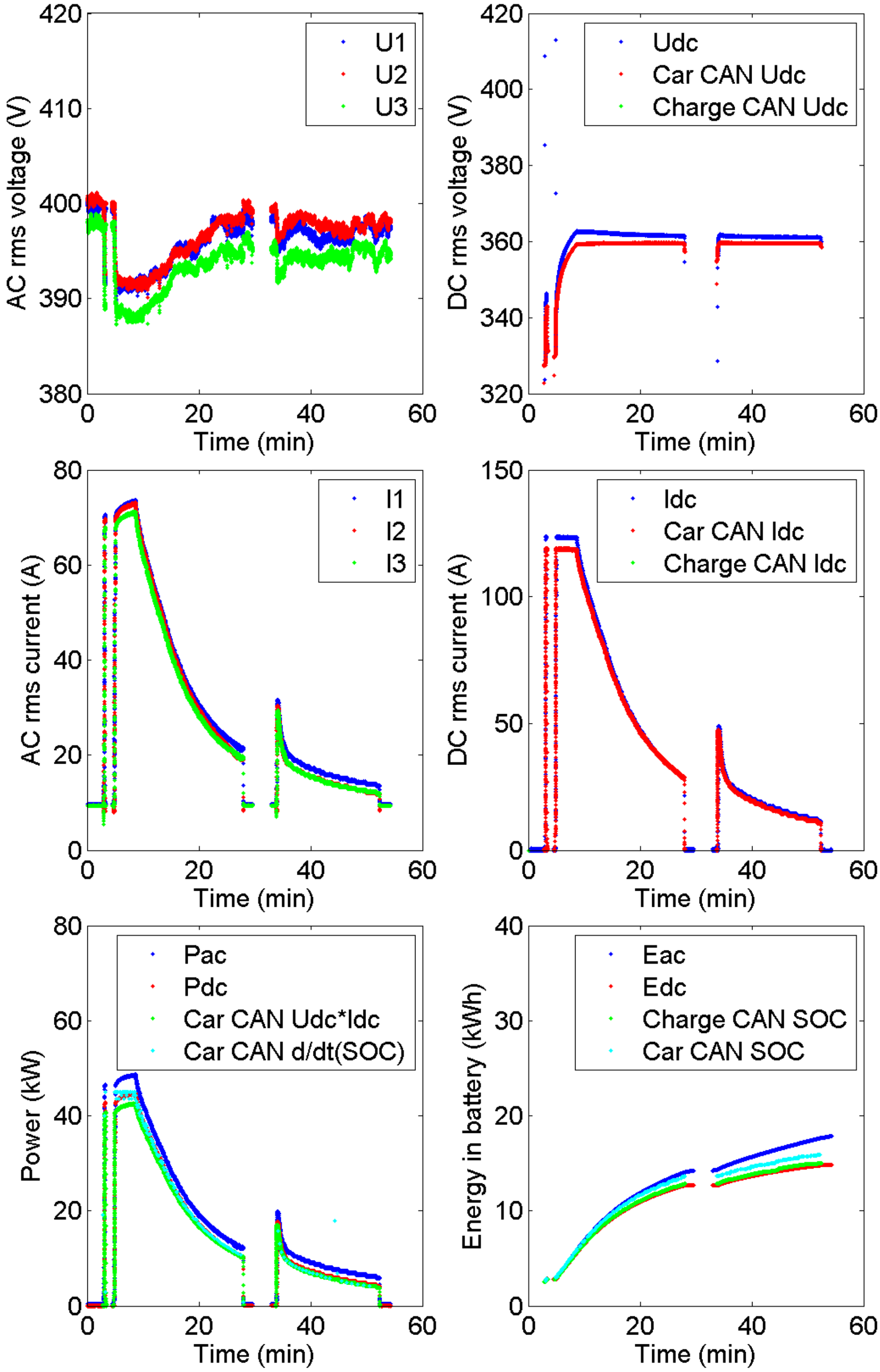

Figure 4.1.1: *Measurement 1: Voltages, currents, powers and state of charge*

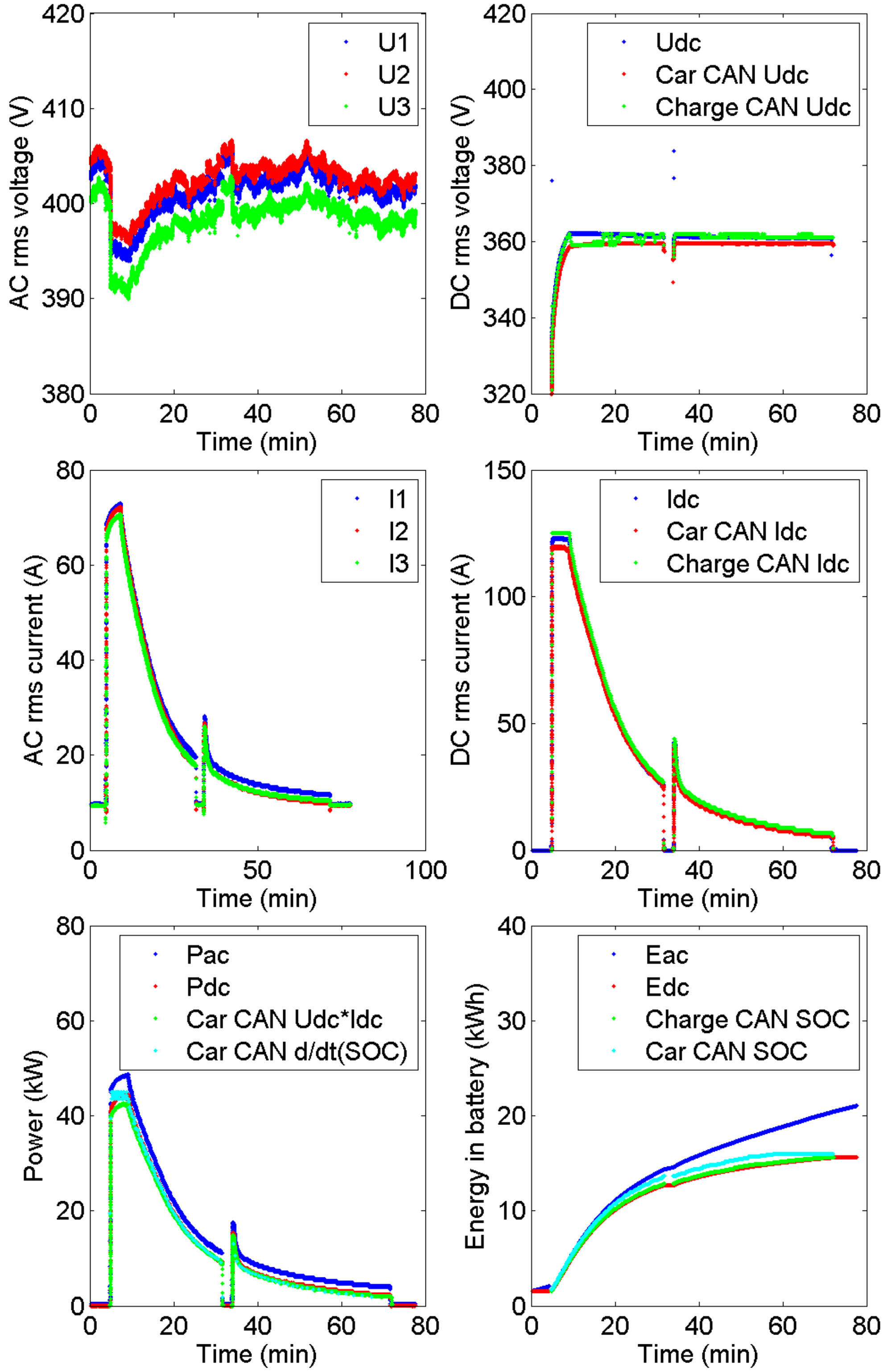

Figure 4.1.2: *Measurement 2: Voltages, currents, powers and state of charge*

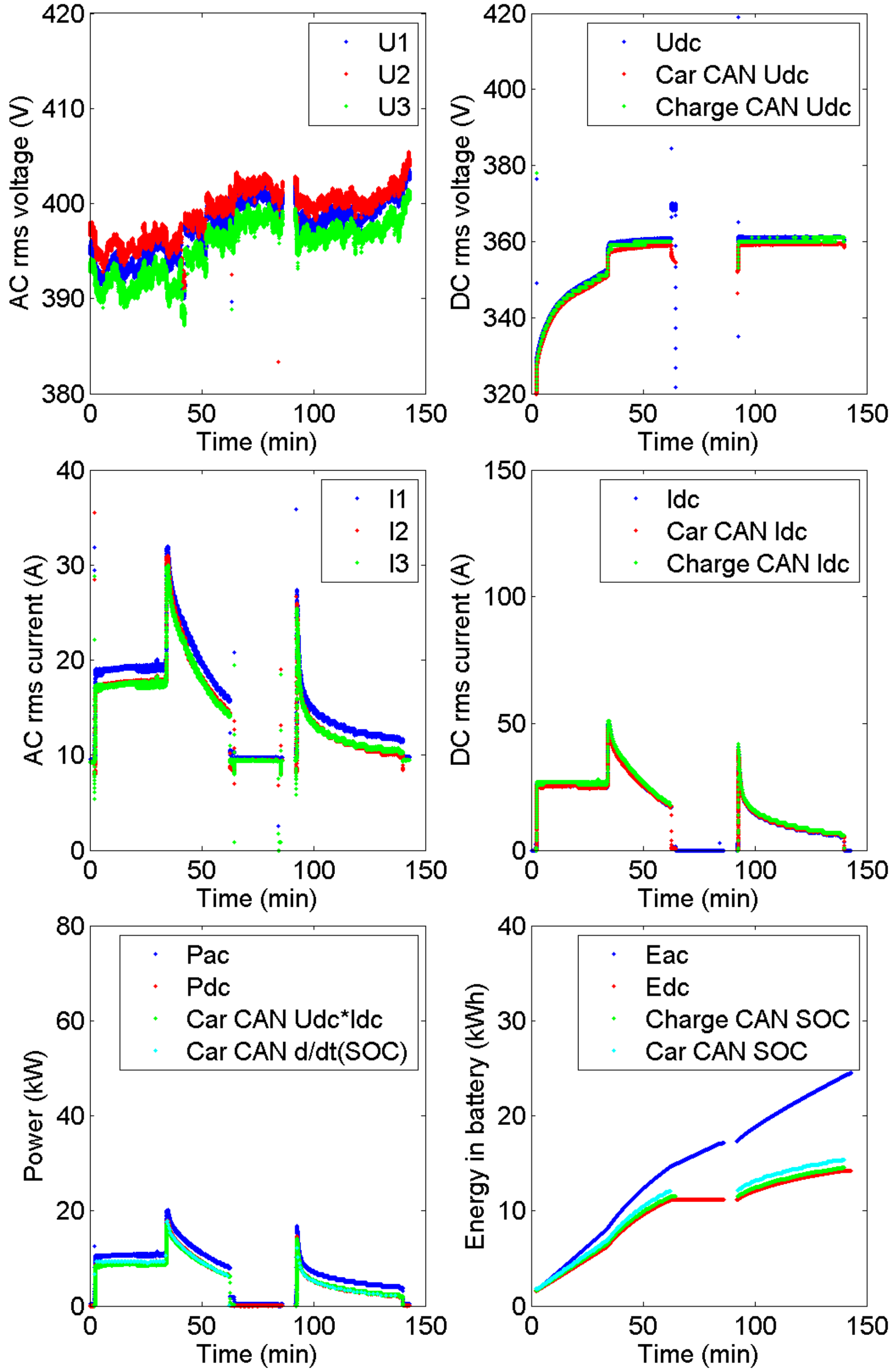

Figure 4.1.3: *Measurement 3: Voltages, currents, powers and state of charge*

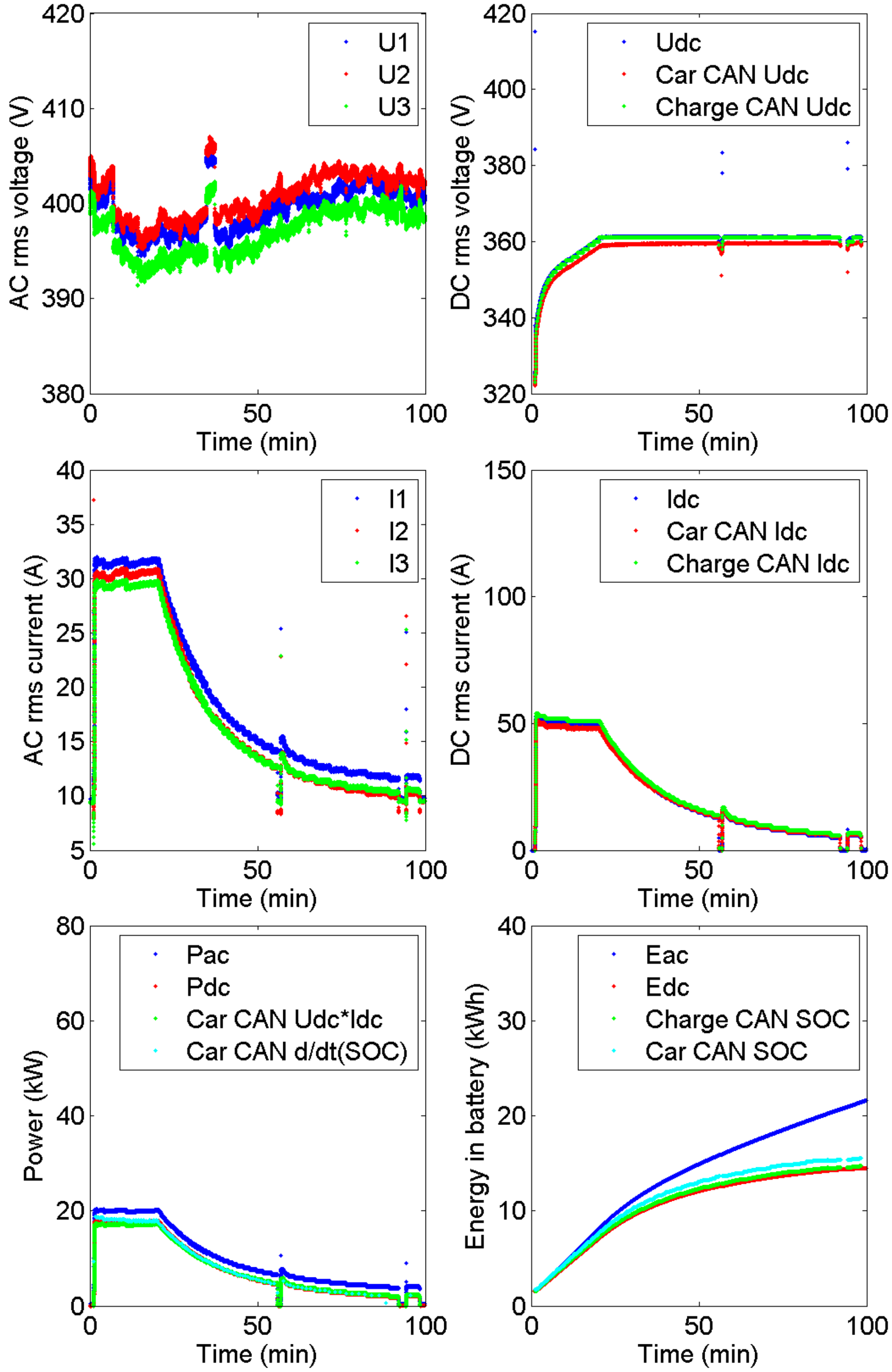

Figure 4.1.4: *Measurement 4: Voltages, currents, powers and state of charge*

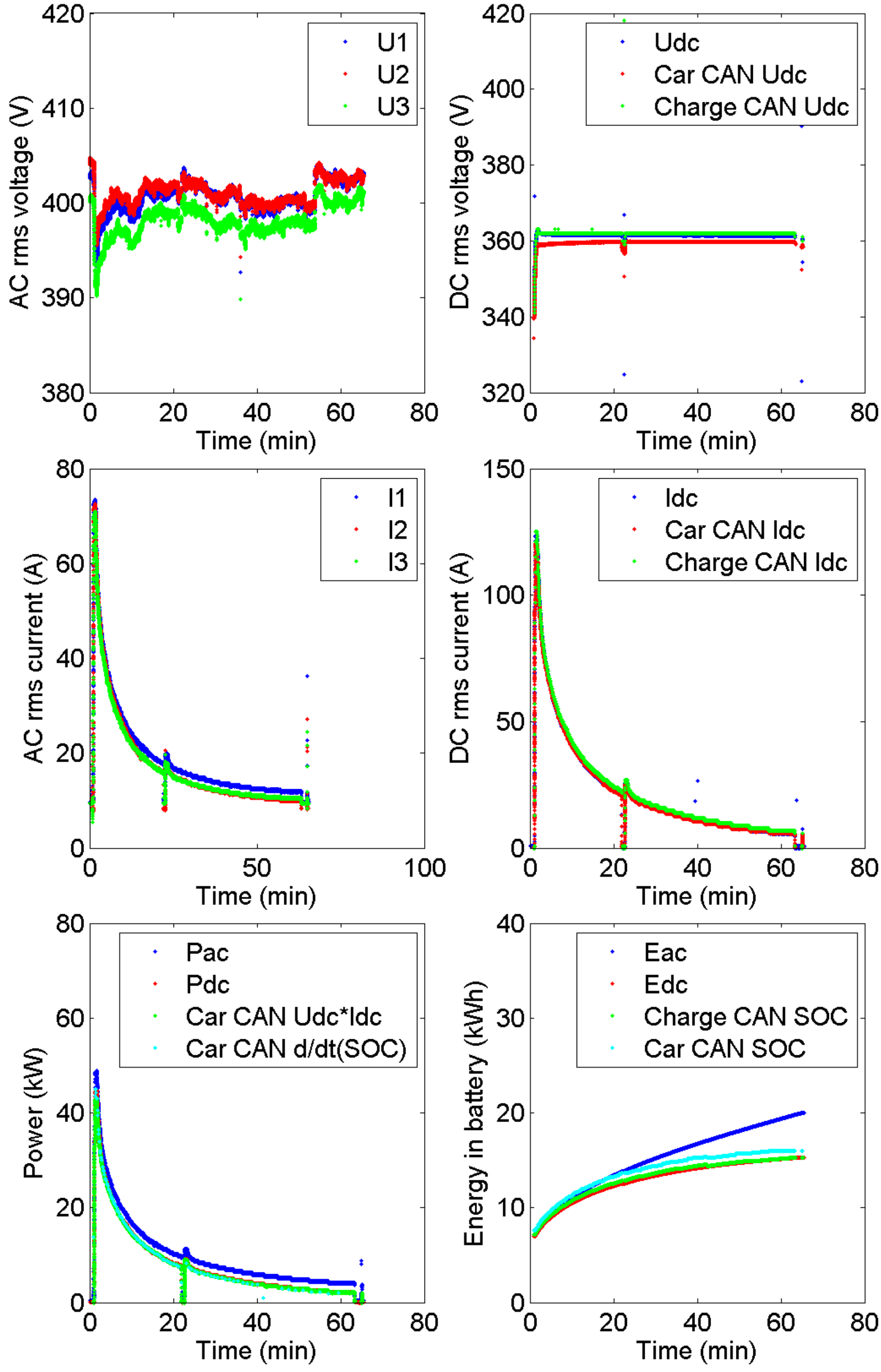

Figure 4.1.5: *Measurement 5: Voltages, currents, powers and state of charge*

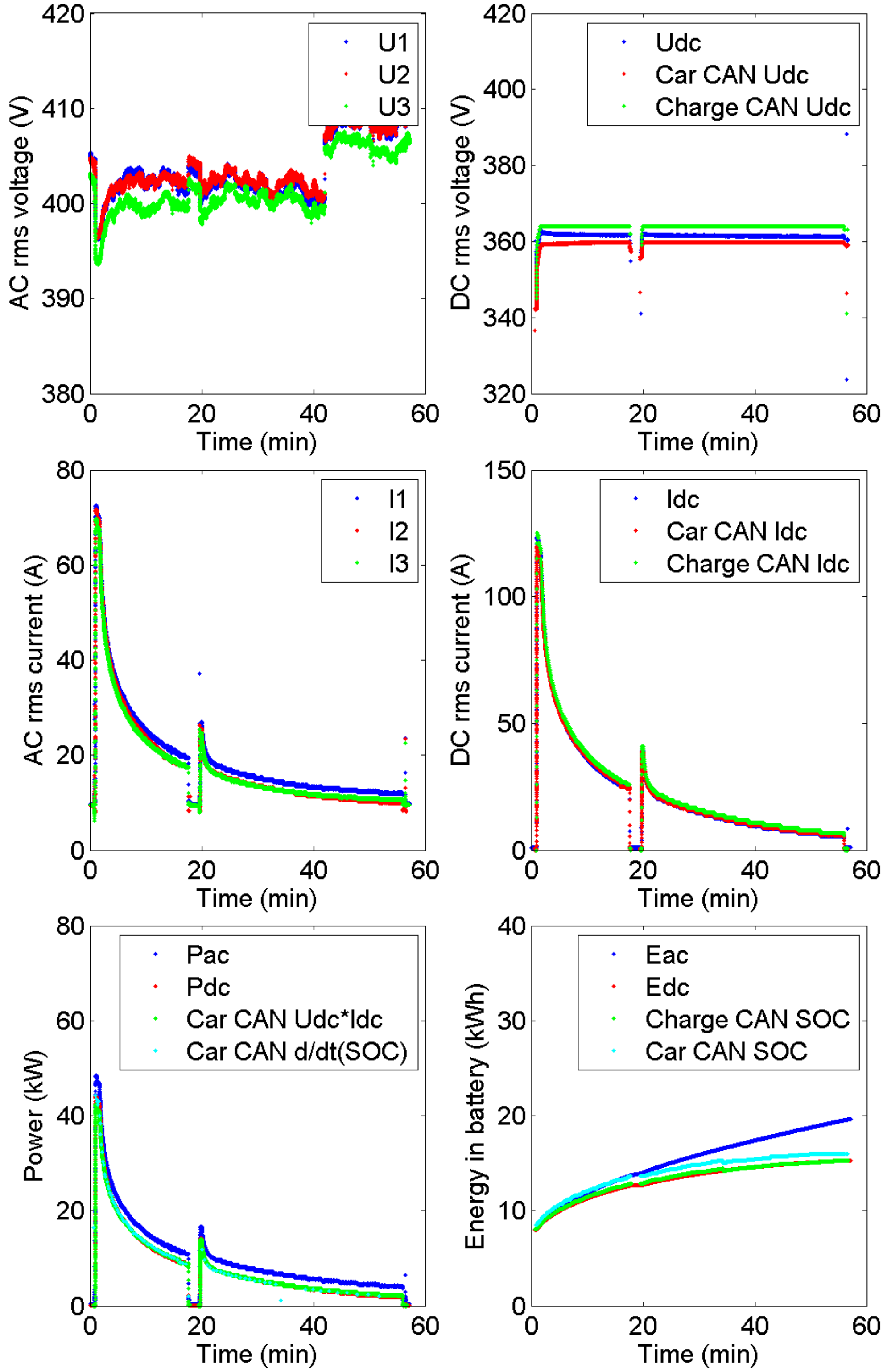

Figure 4.1.6: *Measurement 6: Voltages, currents, powers and state of charge*

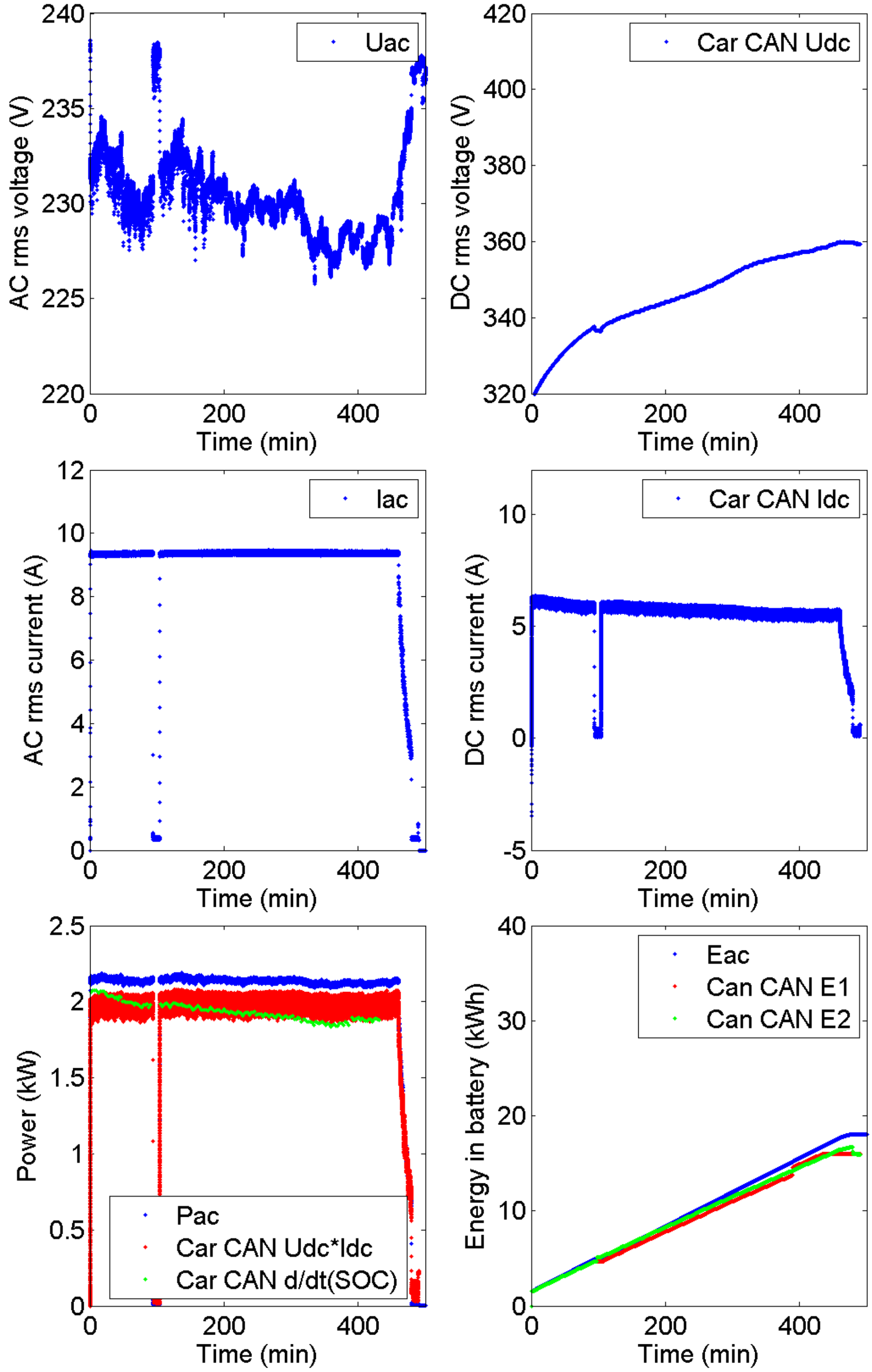

Figure 4.1.7: *Measurement on AC charging: Voltages, currents, powers and state of charge*

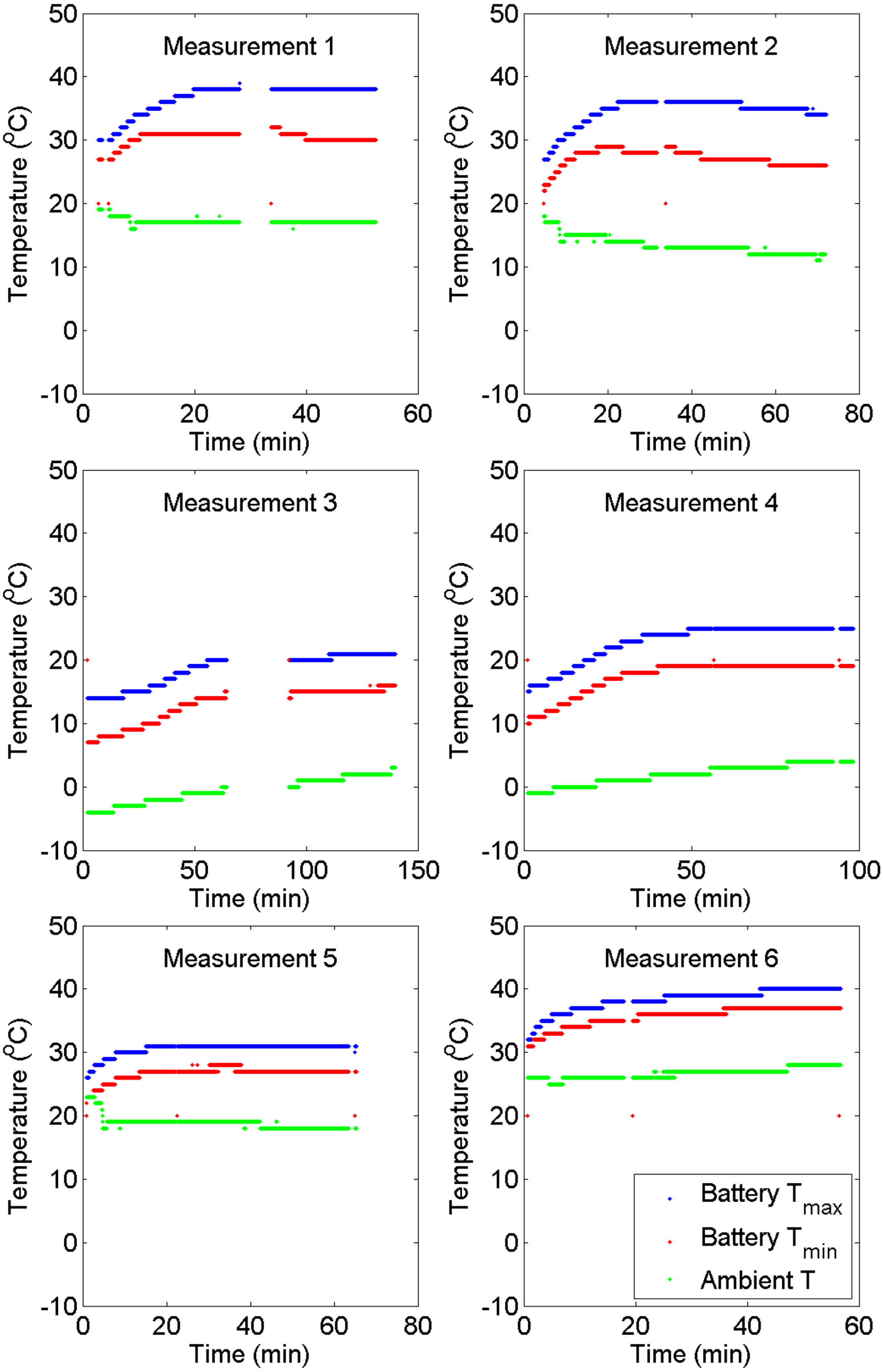

Figure 4.1.8: *Battery and ambient temperature for measurements 1-6*

temperature variation can be found in Figure 4.1.8.

When the charging starts the DC current increases in steps of 3 A to 124A in six seconds and then becomes constant. The DC voltage jumps to 329V and during the increase in current the voltage increases to 343V. During constant current the voltage increases slower, with 0.25V/s.

The AC voltage on the grid dips 10V when the charging starts due to the weak electric grid and high current drawn from the charger. When the current decreases, the voltage increases to its original value. After a few seconds the charger is then stopped manually in order to validate that everything was working.

When the charging is started the second time, the behavior is similar to the previous. The battery is charged with constant current for 4 minutes and the voltage increases exponential to 363V. The battery is then charged with constant voltage and the current decreases exponential in steps of 1-2A until the charging stops at 29A, after 23 minutes of charging. The battery maximum temperature increases from 30 to 38^{o}C during the constant current charging. A fan is then activated and keeps the battery temperature 38^{o}C or bellow. The battery state of charge is just below 84%. When the charging stops, at 28 minutes in the plot, the CAN traffic stops and after a minute the power analyzer is stopped.

In order to charge the battery to 100% the charging must be restarted manually at 33 minutes. The charging from 84 to 94% with constant voltage takes approximately 45 minutes, about the double as the previous charging from 34 to 85%. When the charging is started the current is 60% higher than it was when the charger turned off. This is because the capacitance in the battery needs to be recharged when the charging starts. The current then decreases exponentially from 49 to 11A.

In the bottom right plot in Figure 4.1.1 the energy is plotted. The difference between Eac and Edc is the efficiency of the charger. Eac is how much energy the fast charger has consumed by the grid and Udc is how much energy has been supplied to the vehicle. For more explanations about the differences in CAN and power analyzer data, refer to section CAN verses power analyser.

4.1.2 Measurement 2: warm battery pack

The second measurement is also performed on a warm battery pack. The purpose is to verify the first measurement. The trip mileage counter displayed 1km until the battery is empty.

Figure 4.1.2 illustrates the same parameters as last Figure and the plots are similar to measurement 1. This time the charging to 80% takes 2 more minutes because of the lower initial state of charge. The second part of the charging takes approximately the same time. The maximum battery temperature is 3^{o}C lower and increases to 36^{o}C compared to measurement 1.

4.1.3 Measurement 3: cold battery pack

This measurement is performed with a cold battery pack and the car has been idle for the last 20 hours over the night with ambient temperature below zero. The purpose is to consider the temperature aspect and the time the trip mileage counter displayed 0km. In the beginning the ambient temperature is -4^{o}C and increases to 4^{o}C at the end of the charging, Figure 4.1.3. The battery temperature is between 7 to 14^{o}C when the charging starts. The fact that it is not lower due to the low ambient temperature is the large mass and isolation of the battery.

Figure 4.1.3 visualizes measurement three in the same structure as in previous measurements. Because of the cold battery temperature the charging current is limited to 25A. A measurement the following day with warm battery and same ambient temperature verifies that it is the battery temperature and not the ambient temperature which determines the current limitation. The measurement is not presented in the report due to corrupt in the measurement files. The AC voltage dips only 4V this time. This because with the low initial current, which has a constant value of 18A but now with duration of 40 minutes. For the DC side the voltage increases inverse exponential.

After 40 minutes of fast charging the DC voltage has increased to its predetermined value of 360V. This adjustment to constant voltage triggers a rapid rise in the current to 50A. But the charging current is probably still limited by the temperature. After a few minutes the current starts to ramp down exponentially. When the fast charging time reaches 60 minutes an unexpected error occurs, so the charging process shuts down. 25 minutes after the fault occur the charger is manually activated again so the charging process continuous as in previous measurement. Because of the lower current the charging takes approximately twice as long time.

4.1.4 Measurement 4: cold battery pack

Measurement four is the second measurement with a cold battery pack and it is performed to be able to compare and confirm measurement three. The trip mileage counter displays 0km left. The initial ambient temperature is -1^{o}C , 3^{o}C higher than last measurement and the lowest temperature on the battery is 10^{o}C. This sets the current limitation to 50A instead of 25A as in the previous measurement. Figure 4.1.4 visualizes the measured quantities. The DC voltage increases inverse exponentially meanwhile the DC current is on constant value. This time the current is constant in short intervals it starts on 55A and after few minutes it has decreased to 50A. 20 minutes from start the voltage has reached its constant value of 360V and the DC current starts to decrease exponentially.

After 55 minutes of fast charging the battery has reached 80% of its state of charge, a few minutes after the charging starts manually. When the time reaches 90 minutes the charging is finished but a test to restart the fast charging a third is performed. The charge is start again but as the graph shows it only works for few minutes then the charger automatically turns off. As can be seen in the graph, the AC voltage suffer of a disturbance, which probably comes from the grid.

4.1.5 Measurement 5: half discharged battery

As a final case the battery is discharged to 55%. This time the constant current charging last less than a minute due to the voltage reaches its maximum fast. The first charging cycle takes 21 minutes which is only 4 minutes shorter than measurement 2 where the battery is discharged to 28%. As can be seen in Figure 4.1.5 the plots is similar to the first two measurements but with very short constant current charging.

4.1.6 Measurement 6: half discharged battery

The last measurement is performed to confirm measurement five and the results presented in Figure 4.1.6 confirms the charging behavior. The ambient temperature is 26^{o}C making the battery warmer than in previous measurements, the maximum temperature is 40^{o}C.

4.1.7 Measurement 7: AC charging with 10 A

In order to compare DC charging with AC charging a measurement is performed when the vehicle is charged with 10A trough the one phase AC connector. The charging takes a bit more than 8 hours and the result can be seen in Figure 4.1.7. The charging current to the battery is 3-4A and the charging is performed with constant current for almost the whole charging, only for the last 10 minutes the current is decreased in step towards zero. After 100 minutes the charging is stopped for 10 minutes and during that time one of the values for the battery state of charge increases momentarily 2.4 percent units. This is possible due to that the sensor is calibrated when the charging is stopped, but this has not been verified since detailed technical information is confidential.

4.2 Charging behavior

In order to compare the different measurements, the time axis is normalized by plotting the desired quantities with respect to battery state of charge or DC power. Notice that the time and battery state of charge has no linear relationship but exponential, i.e. when a quantity is plotted with respect to state of charge the corresponding time is fast at the beginning and slower at the end. For example compare the DC voltage and currents in Figure 4.1.1 with Figure 4.2.1.

4.2.1 Voltage and current characteristic of charging

The charging starts with constant current and when the voltage reaches 360V the current starts do decrease and the voltage is constant, Figure 4.2.1. The missing part from the slow charge is because the state of charge is calibrated up at 14kWh (88%).

Because of the lower charging current in measurement 3 and 5 it takes longer time for the voltage to reach its maximum. When the current is lower the voltage is also lower, this is because the resistance in the battery. The voltage in the normal charge with 10A is close to the battery characteristic defined as open source voltage V_{OC} as function of battery state of charge $V_{OC}(SOC)$. This is also confirmed by the initial voltages from the fast charging measurements seen the lower plot in Figure 4.2.1.

When the battery state of charge reaches 12.8kWh (83%) (11.2kWh (76%) for measurement 3) the charging stops and must be restarted manually. This can be seen in the plot as the vertical lines. When the charging continues the current becomes higher than before but stops after some minutes and follows the same asymptote as before. This is because the capacitance behavior of the battery.

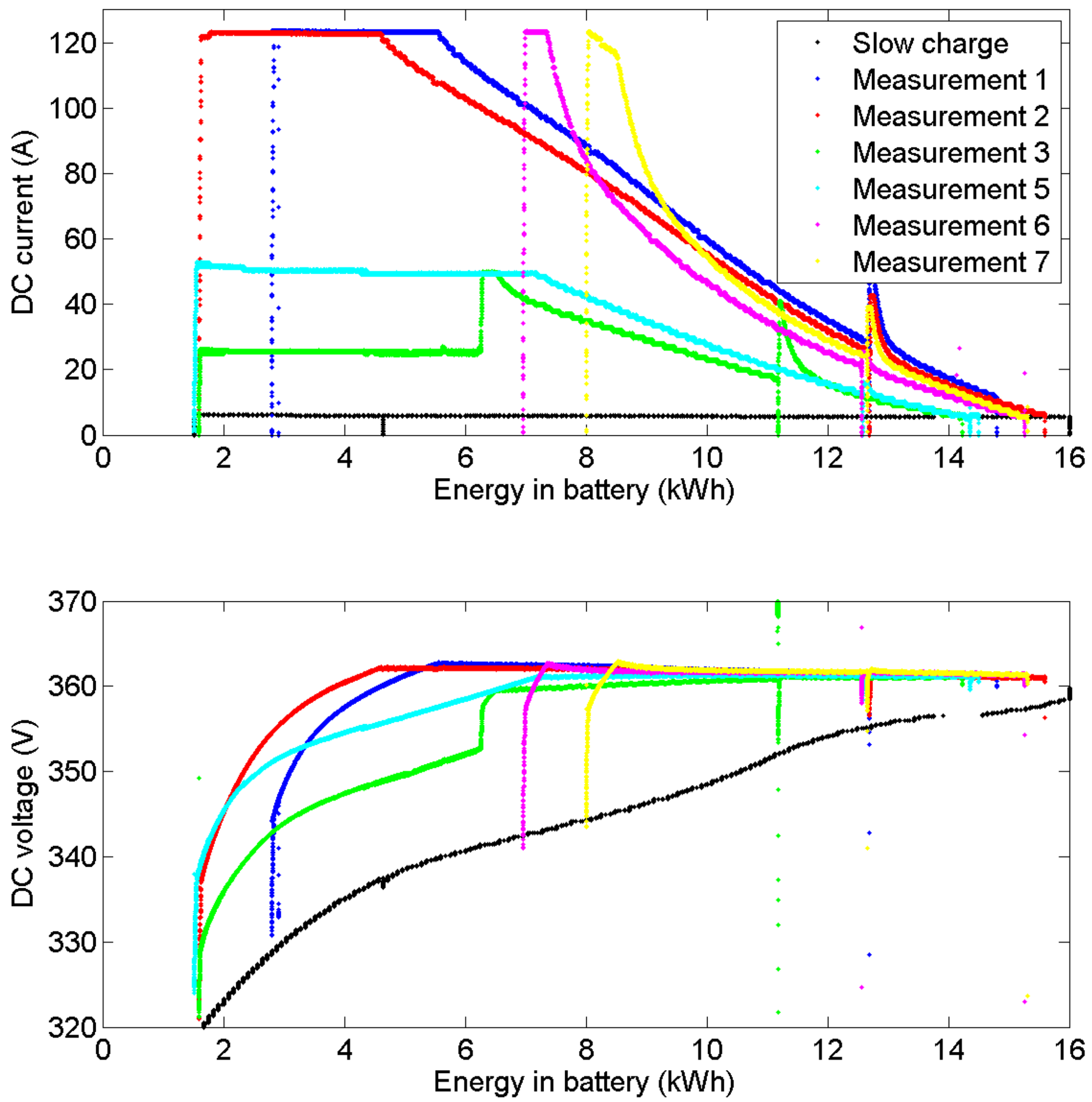

Figure 4.2.1: *DC voltage and current as a function of battery state of charge*

4.2.2 Battery resistance

By taking the momentarily voltage increase at the start of the charging divided by the starting current in Figure 4.2.1 the impedance of the battery can be estimated for the six measurements on the fast charger:

$$
\begin{aligned}
(344 - 331)/123.5 &= 0.1053\Omega \\
(337 - 321)/121.5 &= 0.1317\Omega \\
(329 - 321)/25.0 &= 0.3200\Omega \\
(337 - 324)/52.0 &= 0.2500\Omega \\
(357 - 341)/123.0 &= 0.1301\Omega \\
(357 - 343)/123.0 &= 0.1138\Omega
\end{aligned}
$$

The calculated resistance varies between 100 to 320mΩ, the variation is probably because of reading error in the figure. The value given in the datasheet is 132mΩ which is within the reading range for the voltage and current in the figure.

4.2.3 Temperature dependence

The battery management system in the car limits the current depending on the battery temperature in order to not damage the battery cells. This can be seen by comparing the battery temperature in Table 4.1.1 with the currents in Figure. 4.2.1. In measurement 1 and 2 the battery temperature is 22 - 30^{o}C and the battery request maximum current of 125A. When the battery is cooler in measurement 3 and 5 the current is limited to 25 respective 50A, battery temperature in this cases 7 to 14 respective 10 to 15^{o}C. The current is also limited in measurement 3 when the charging switches from constant current to constant voltage at t=52min. In this case the battery temperature has increased and allows a higher charging current. The voltage is also lower when charging with lower currents, this can be seen in Figure. 4.2.1. This is due to the lower current which makes the increases in voltage slower. The results from the different measurements can be found in Table 4.2.1.

Table 4.2.1: Approximate temperature dependence of charging current

Approximate temperature	Charging current
$< 10^oC$	25A
$10 - 20^oC$	50A
$> 20^oC$	125A (rated)

4.2.4 Charger efficiency

The output power in Figure 4.2.2 is similar to the current characteristic. Because of the constant current and voltage increase the power increases during the constant current phase of the charging. It can also be seen that the fast charging does not charge the battery to the maximum but only to 14.2 to 15.6kWh (88.75 to 97.50% of maximum state of charge).

The lower plot in Figure 4.2.2 relates the efficiency of the charger with the battery state of charge. As can be seen the efficiency is above 90% when the battery state of charge is below 70% and the battery is warm (measurement 1 and 2). When the battery is cold the efficiency is 88% for 50A load current 82% for 25A load current. This means that the fast charger is optimized for the full load current (125A) and warm battery. When the state of charge is 83%

(76% for measurement 3) the charging stops and need to be restarted manually in order to continue charging. In this second charging cycle the fast charger's efficiency decreases from 85% to 50%.

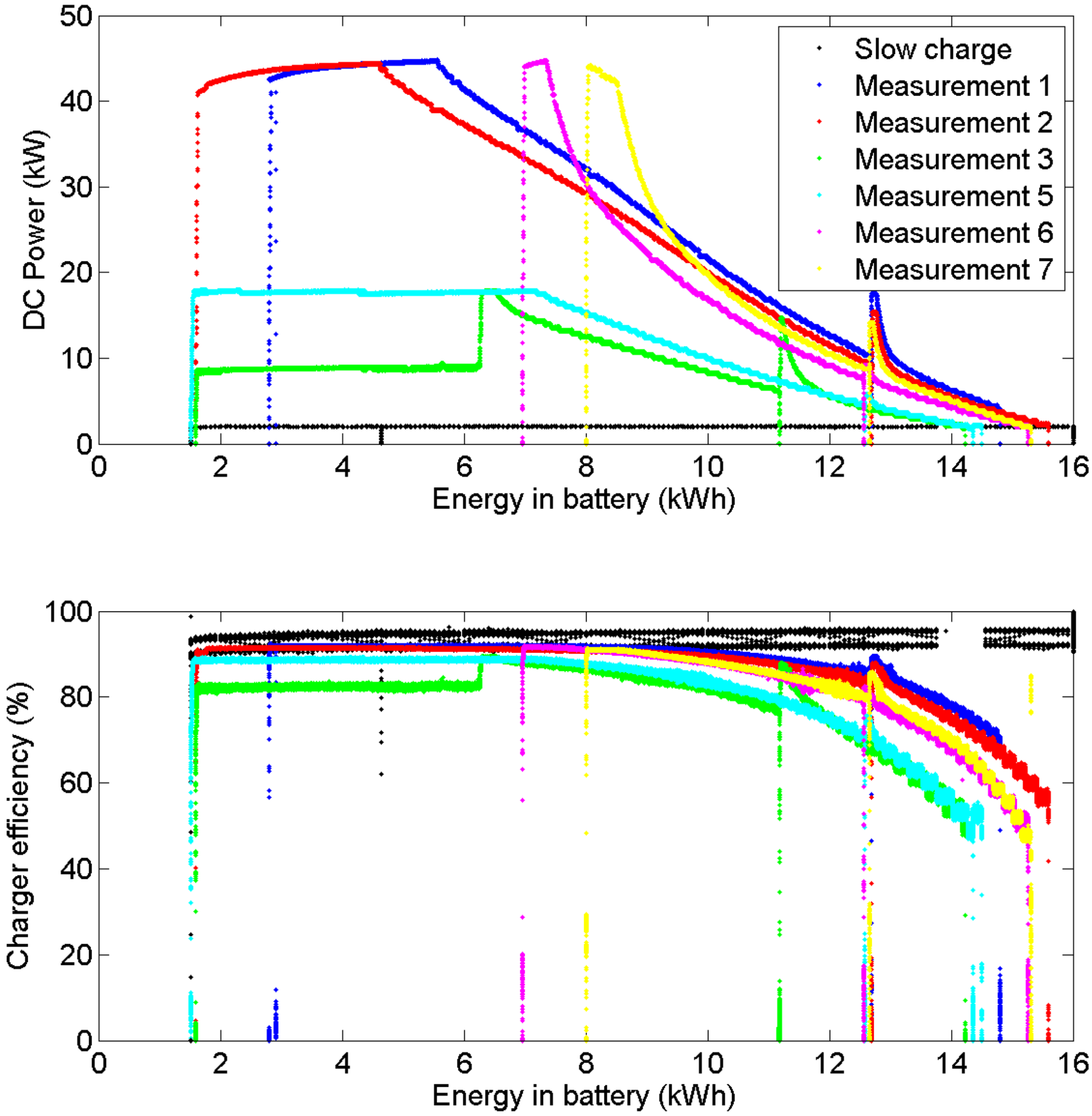

Figure 4.2.2: *Charger power output and efficiency as function of state of charge*

Onboard AC charger

The power of the AC charging is 2kW during the whole charging, Figure 4.2.2. The efficiency of the AC charger is higher than the fast charger for all state of charge but it is first at levels above 60% or 9.6kWh battery state of charge the difference is increasing a lot. The efficiency the charging is between 90-96%. The range of the charger depends on the fluctuation in the

DC current seen in Figure 4.1.7 and the fluctuation is magnified in the power due to the multiplication with voltage. This can also be seen the lower plot in Figure 4.2.3 where the efficiency alternates 91 to 95%.

4.2.5 Charger and battery efficiency

In Figure 4.2.3 the relative efficiency of the fast and slow chargers are plotted and in Figure 4.2.4 the absolute losses in the chargers can be seen. At full load the fast charger has efficiency between 91-92% which corresponds to 4kW in losses. When the load decreases below 20kW the efficiency decreases below 90% (approximately 2kW in losses). When the output power decreases even more the efficiency decreases towards zero. At 2kW output power the efficiency has dropped to 50%. The slow charger has an efficiency of above 90% and losses between 100-200W.

The losses in the battery is quadratic to the charging current due to $P = IR^2$ and can be found in the lower plots in Figures 4.2.3 and 4.2.4. As can be seen the maximum battery losses is 50% of the charger losses at rated power of 50kW which corresponds to an efficiency of 95.5%. During slow charge the losses in the battery is less than 5W. The losses in the battery heats up the battery which can be seen in Figure 4.1.8.

4.2.6 CAN verses power analyser

As can be seen in Figure 4.1.1 to 4.1.6 there is a difference in the quantities measured by the power analyzer and the vehicle. In the last four measurements the charge CAN voltage is some volts higher than the voltage measured by the power analyzer and the Car CAN some volts lower. This can either be because of measurement errors or by the voltages are measured on different location i.e. a part of the power is fed to other parts in the vehicle and not the battery. In presentations found about CHAdeMO the battery management system in the vehicle request a voltage and the fast charger only delivers that voltage, which would explain that the charge CAN voltage is higher than the voltage measured by the power analyzer. The vehicle CAN voltage is probably measured close to the battery and the vehicle needs some hundred watt of powering the computers. This can explain that this voltage is lower. The same reasoning can be applied for the currents.

4.3 Power quality

Because of the weak grid surrounding the fast charging station in Agnesberg and the large power drawn by the fast charger different phenomena related to power quality can be seen on the electric grid.

4.3.1 Harmonics

Figure 4.3.1 presents the Fourier transform of the RMS voltage and current for three different DC currents when the fast charger is: powered off, delivering maximum current of 125A, and delivering currents below 10A. The power analyzer measures the first 100 harmonics and it is only the change of the harmonics which are of interest. Most of the harmonics are not created by the fast charger but rather from other equipment in the grid. Most significant is

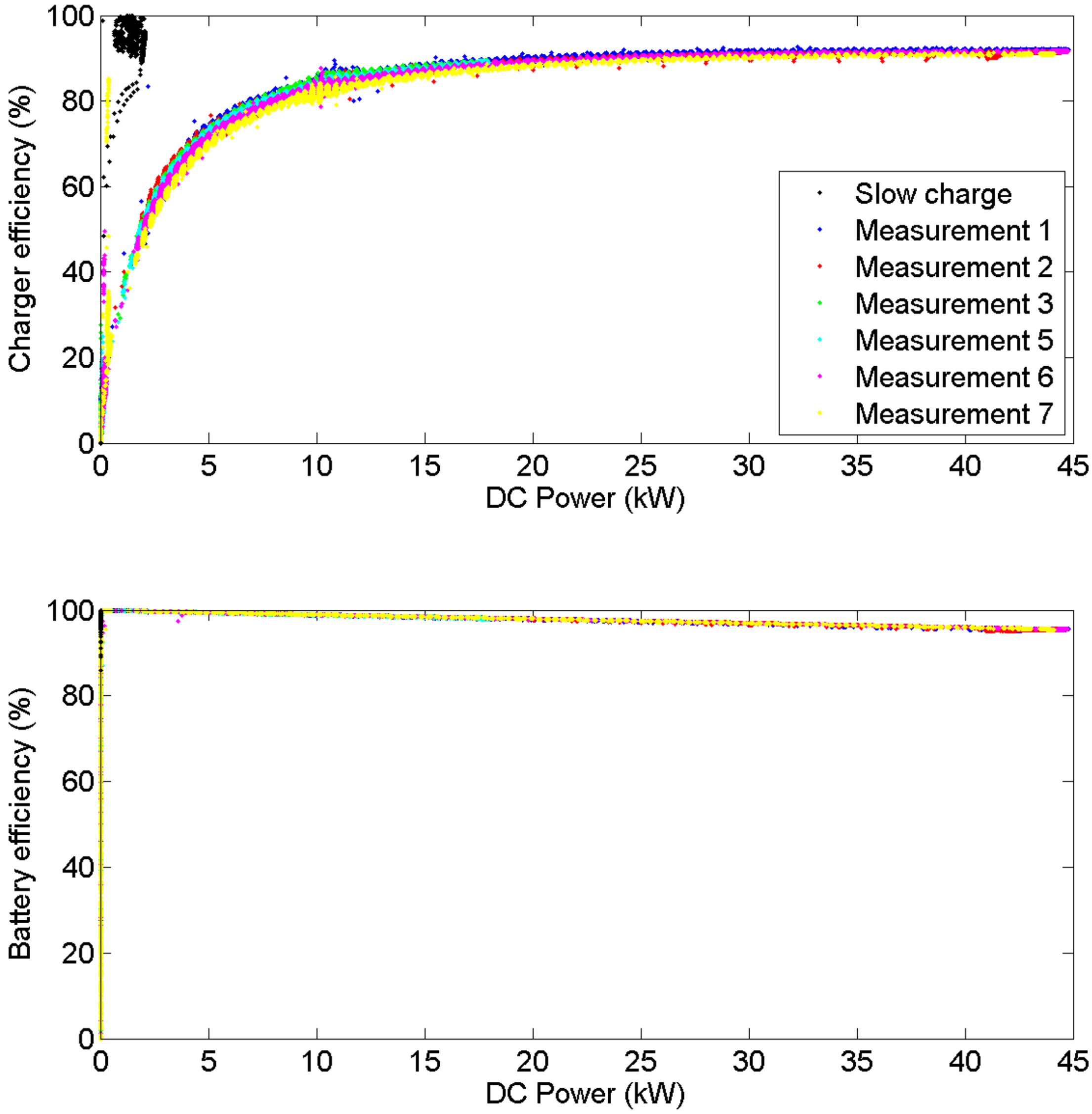

Figure 4.2.3: *Converter and battery efficiency as a function of DC power*

the sideband of the switching frequency of 4kHz in both voltages and currents. In order to make the result a bit more clear the first 20 harmonics is presented in Figure 4.3.2. In the voltage the first harmonics is almost the same and the 11^{th} and 13^{th} are decreased when the fast charger is operating. All of the harmonics is lower than 1% of the rating 400V. The current harmonics increase with higher charging current except for the 11^{th} harmonic which decreases. All current harmonics is lower than 2% of rated current at 120A.

Figure 4.3.3 and 4.3.4 visualize how the five dominant harmonics and total demand distortion (TDD) are varying during measurement 2 and 3. The thin black line is the DC current scaled to fit in the plot. When the charger starts, the voltage harmonics decreases little and the variation during the charge is to small to be related to the consumed current. The total TDD is around or below 1% of the rated voltage 400V which is considered as good power quality.

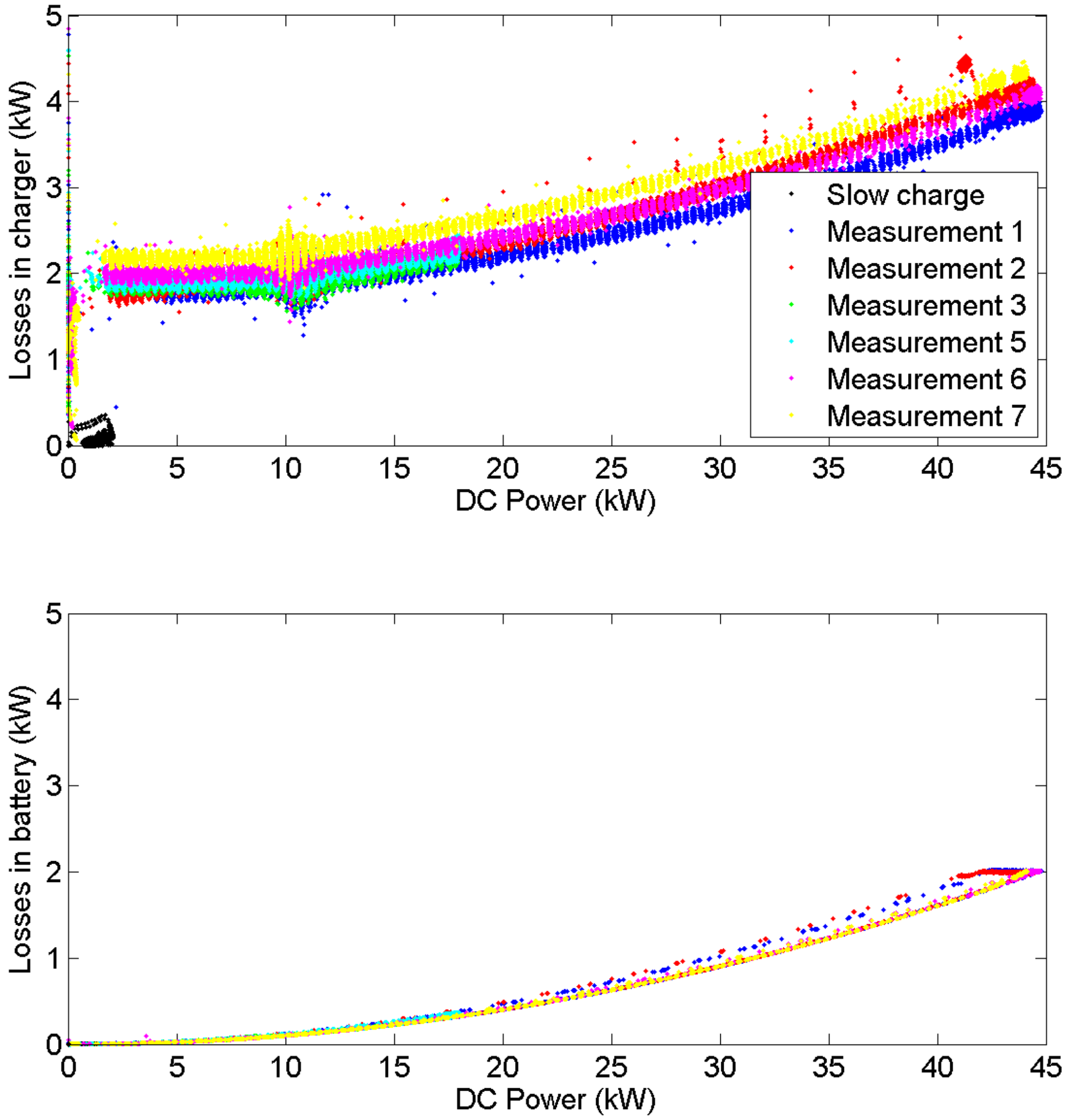

Figure 4.2.4: *Absolute power losses in charger and battery*

The current harmonics in Figure 4.3.3 and 4.3.4 changes during the charging. When the charging start the charger reduces the 13^{th} harmonics by 50% but the 5^{th} and 7^{th} increases which increases the total TDD in the grid. When the power decreases during the charge (propositional the thin black line) the TDD first increases but decreases a again in the end of the first charging cycle. The same behavior can been seen in both measurements why it is reasonable to conclude that it is the charger and not anything else in the grid which gives the harmonics. The TDD is slightly above 2% of rated current 120A as maximum and the charger increases the current harmonics on the grid.

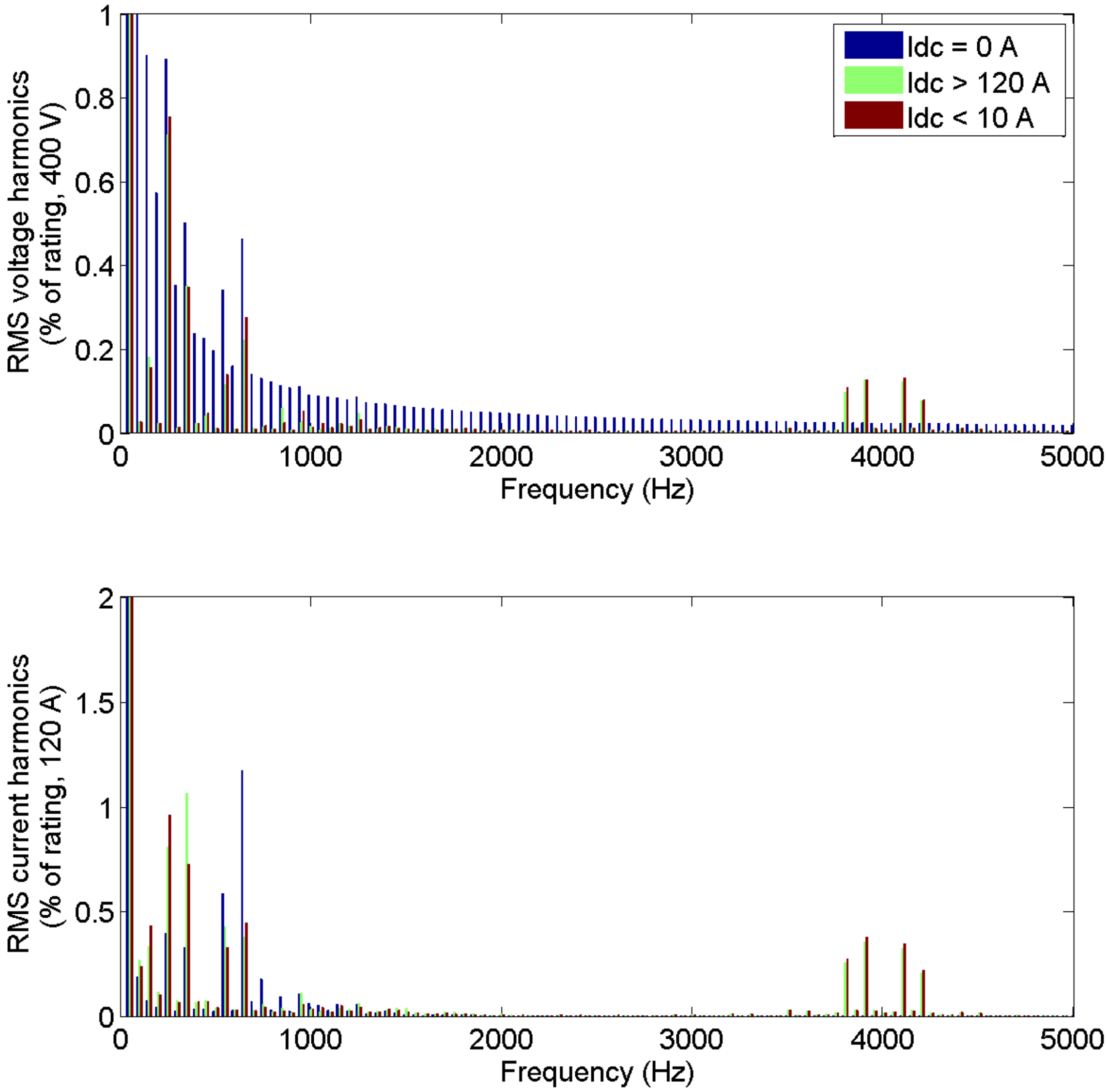

Figure 4.3.1: *Average harmonics for n=0 to 100 in phase 1 for measurement 2*

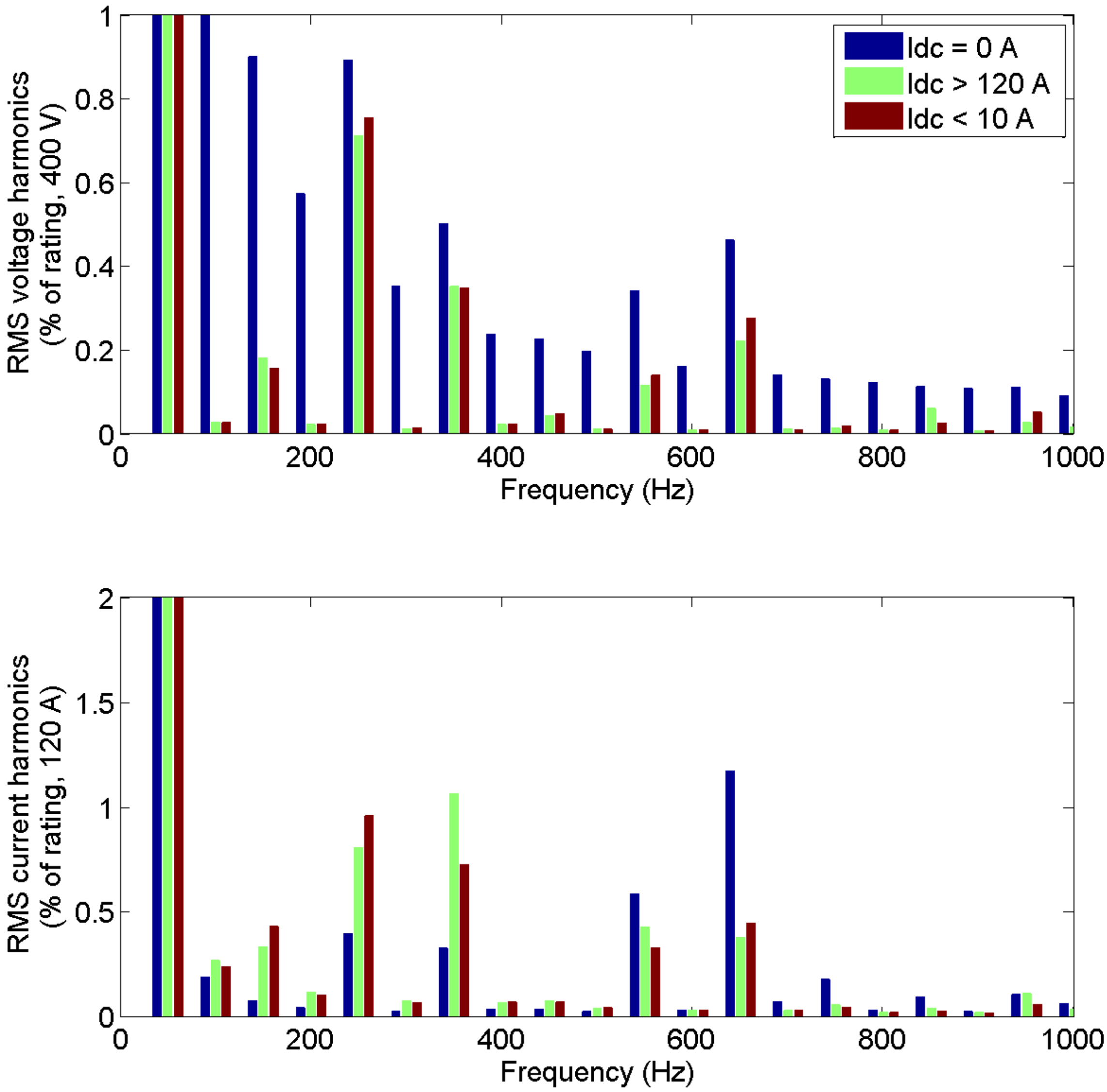

Figure 4.3.2: *Average harmonics for n=0 to 20 in phase 1 for measurement 2*

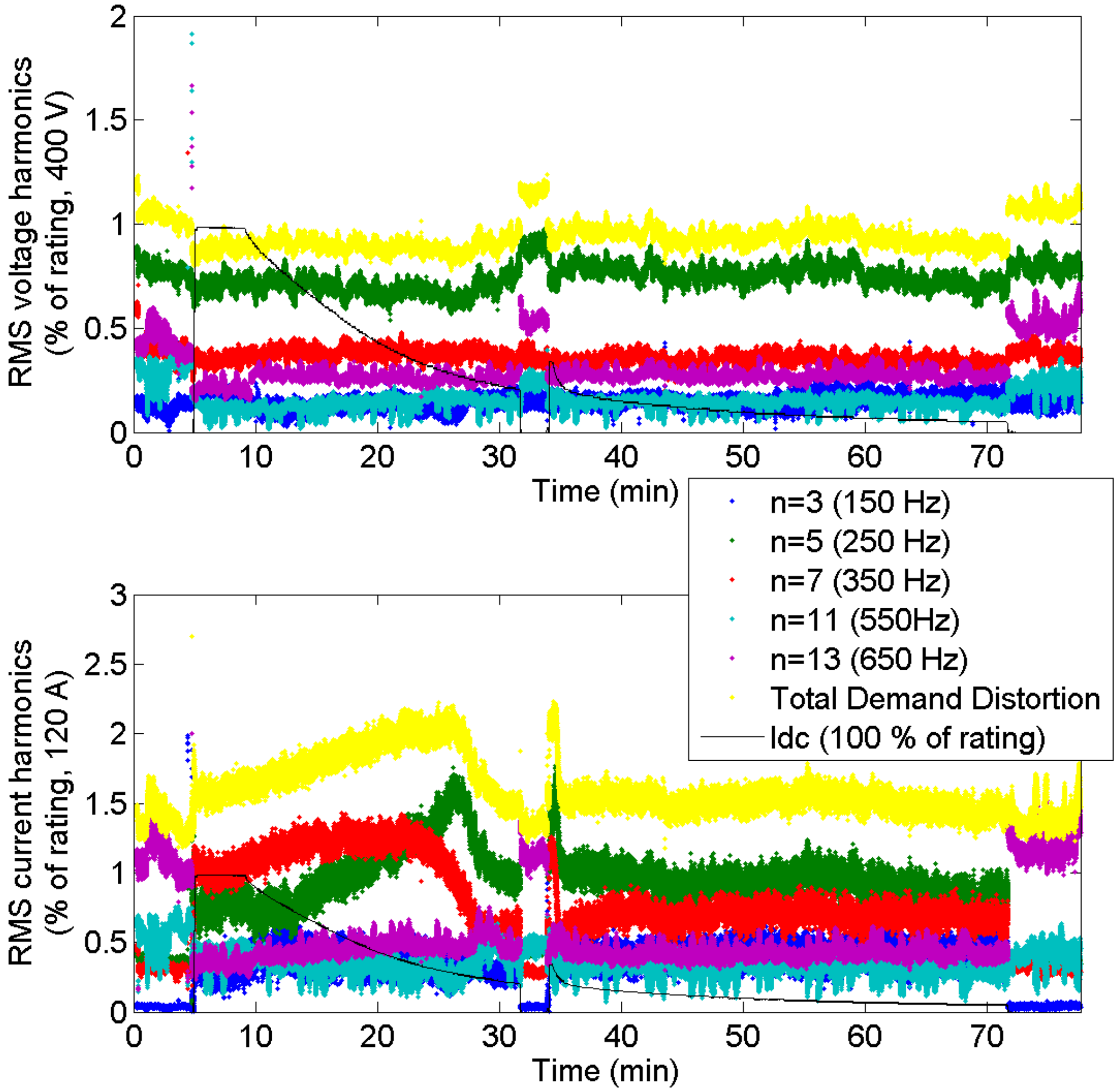

Figure 4.3.3: *Time dependence harmonics for phase 1 for measurement 2*

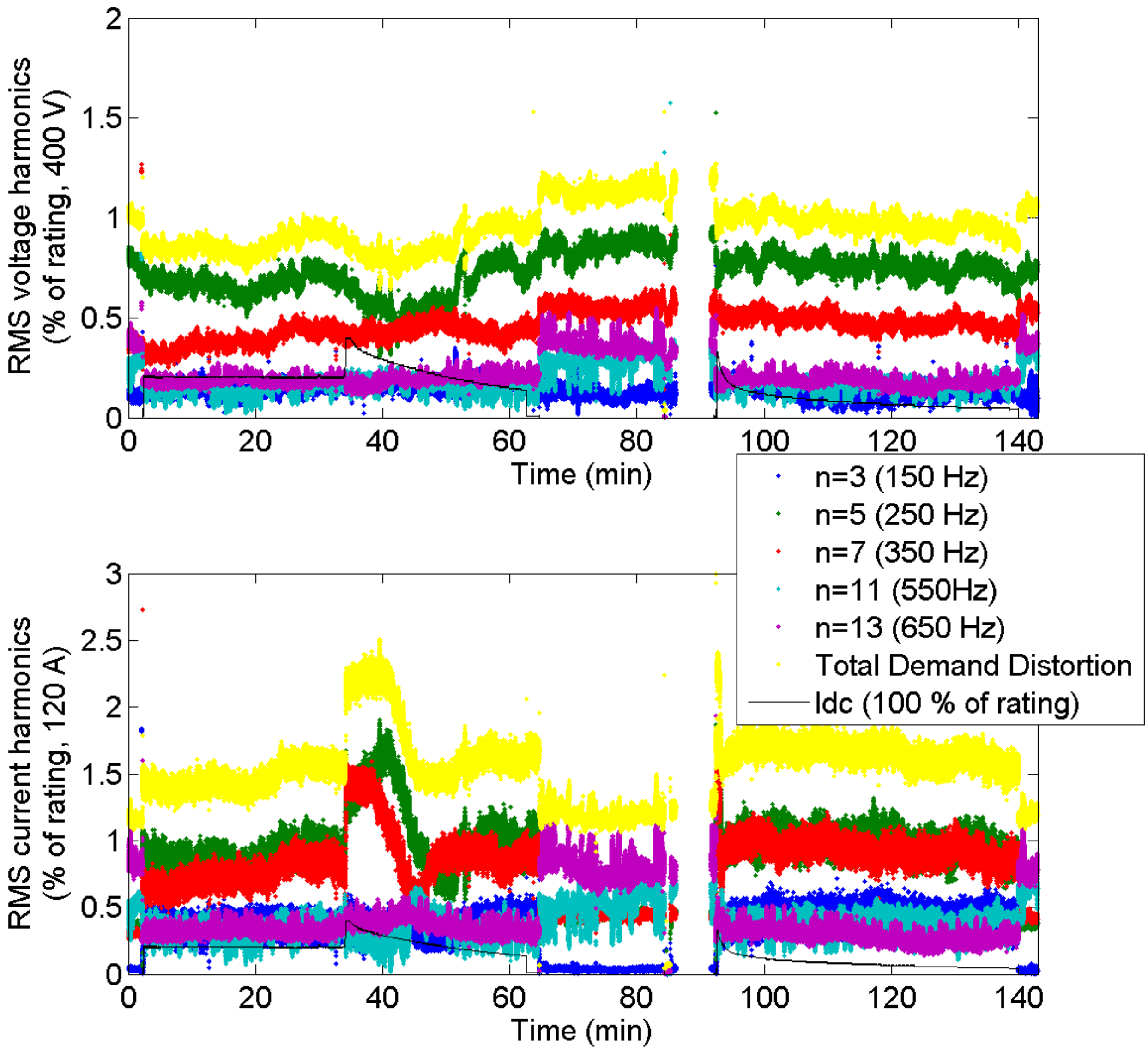

Figure 4.3.4: *Time dependence harmonics for phase 1 for measurement 3*

4.3.2 Voltage dip

When the charging starts, the grid voltage dips, this can be seen in Figure 4.1.1 to 4.1.4. When 70A is consumed by the charger in each phase, the voltage dips with 10V for measurement 1. When the current starts to decrease, the voltage starts to increase to the initial value. In order to compare the different measurements, the grid voltage has been plotted with respect to the grid current, Figure 4.3.5. The relation between the voltage and current is approximately the same. This is due to the slope in the grid impedance, which is characterized by the design of the surrounding grid. The unloaded voltage level (the charger consumes 10A reactive power at no load) varies between the different measurements and are due to other loads and tap changer settings in the surrounding power grid.

From the slope in Figure 4.3.5 the absolute value of the electric grid impedance can be calculated:

$$Z = \frac{405 - 395}{72.5 - 10} = 160m\Omega \tag{4.3.1}$$

By assuming the relationship between current and voltage also for higher current the voltage dip for the rated current of 120A is calculated to $120 \cdot 0.160 = 19.2V$ which is larger than the allowed value of the voltage variations.

4.3.3 Reactive power

At no load the charger consumes 400W active power and produces 6.6kVAr reactive power. Even at small loads, below 5kW, the charger produces 6.6kVAr. This can be seen as the dots to the lower left in the upper plot in Figure 4.3.6. This is probably because of a capacitive filter in the charger[3].

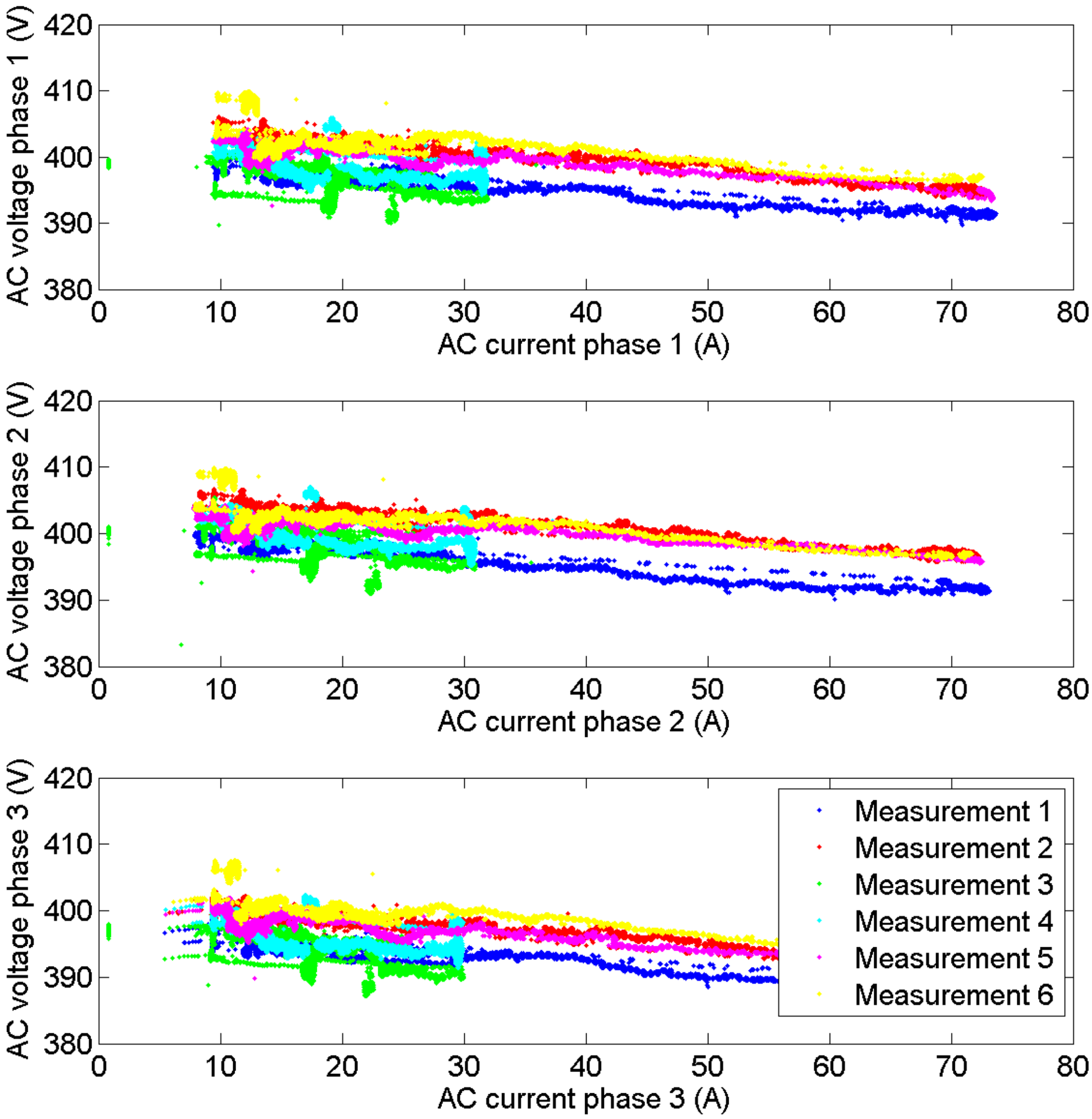

Figure 4.3.5: *AC phase voltage as a function of phase current*

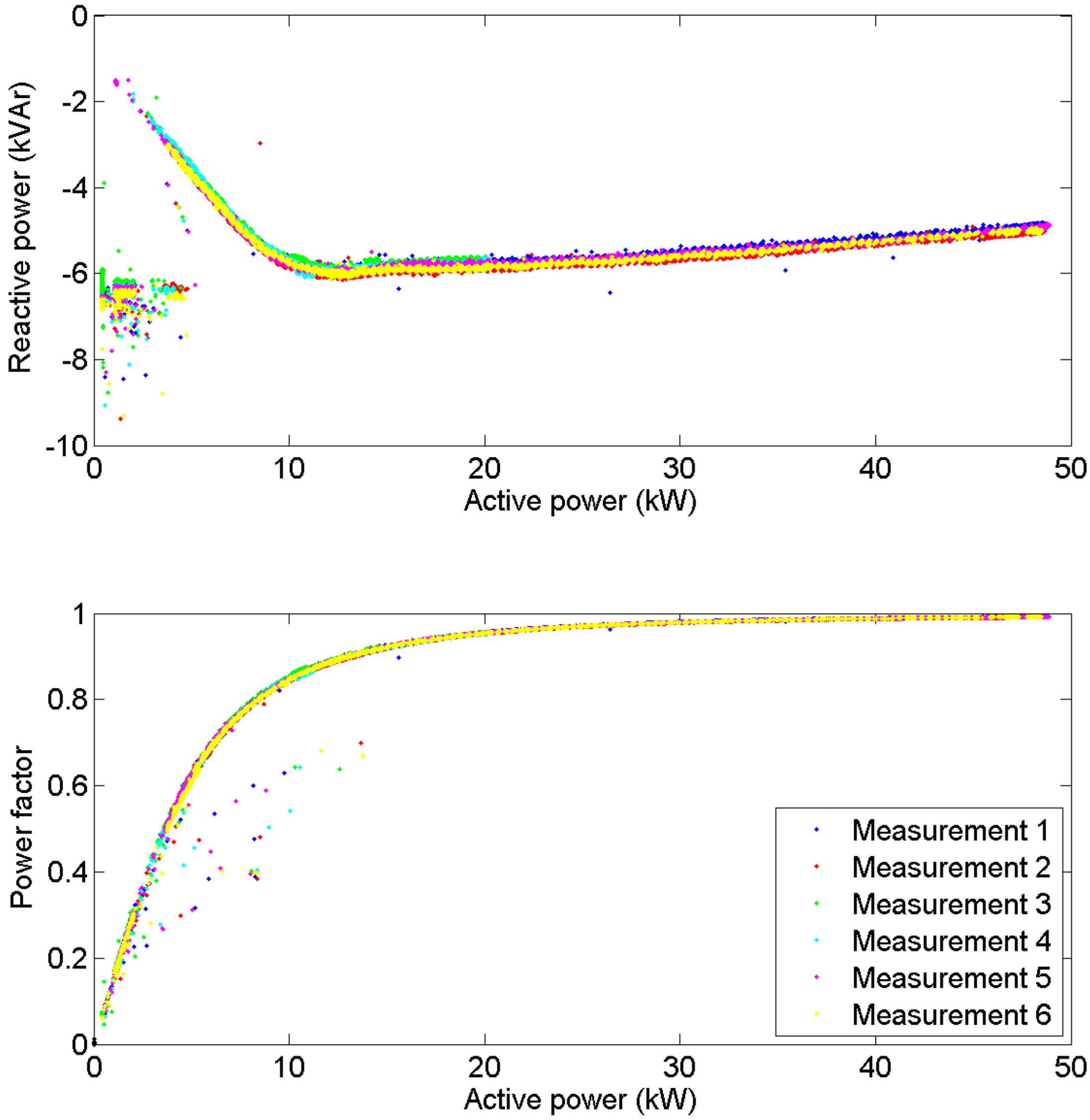

Figure 4.3.6: *Active and reactive power consumed by the charger*

5 Conclusions

In this study it has been shown that the temperature of the battery has not only a high influence of the charging current. The temperature is actually the major condition for setting the charging current, which then determine the charging time. When having ideal conditions such as, battery temperature above 20^oC and 10% state of charge, the fast charging takes only 30 minutes to 80% for a 16kWh battery pack. The power during the first minutes is close to rated power of 50kW and 125A DC current. Between battery temperatures of approximately 10 to 20^oC the charging current is decreased significantly to 50A. When the battery temperature is below approximately 10^oC the charging current decreases further to 25A. As an effect of the lower charging current, the charging time increases to almost the double to 60 minutes for charging to 80% of maximum capacity.

The battery state of charge also influences on the charging time. If a fast charging is performed on a battery pack with a state of charge at 50% and with a battery temperature at 25^oC, the charging current starts on its maximum value 125A. Since the transferred power has an exponential behavior the charging time to a 80% state of charge takes 18 minutes. This concludes that it is more time efficient to charge the battery with lower initial state of charge, because of the higher power at low state of charge.

The measurement performed on the fast charging station provides an idle loss around 400W. For a fast charging station that are built to provide an output power of 50kW it may not be any major issue. By looking for a whole year it comes to consideration, since the losses are 3 504kWh, which corresponds to 219 battery packs with the capacity of 16kWh. This encourage improvements on the fast charging station. It has not been further investigated of where in the fast charger the standby losses are.

A comparison between DC charging and AC charging shows that the AC charging is more efficient. It has efficiency between 90-96% compared to the DC charging, which has an efficiency between 91-92% when the power output is 50kW but when the power output decrease to 2kW the efficiency is around 50%.

The fast charging station is installed in the distribution grid, with the rated main voltage 400V and rated current at 120A. When the charger is activated a voltage dip of 10V is generated and the load current is around 70A.

Harmonics are both generated and cancelled from the fast charging station, the switching frequency is 4kHz, the sidebands are where the harmonics are generated. For the lower harmonics, especially the 11^{th} and 13^{th} harmonics the charger lower the magnitude. The total demand distortion (TDD) for the voltage is below 1% and for the current harmonics the TDD is below 2%.

5.1 Future work

The infrastructure for fast charging stations must be considered. Especially along the highways where the fast charging stations will work as range extenders. By installing fast charging stations within an distance of for example 50km encourage the usage of electric vehicles. It also gives the driver the confidence to use the electric vehicle for longer distance and neutralize concept as range anxiety.

Because of the active rectifier in the fast charger with IGBT it should be possible to use it as an STATCOM even when no vehicle is connected. The STATCOM could be used to regulate the voltage level, power factor control and perhaps reduce low-order harmonics in the grid.

An interesting study for the future is the user behavior, especially when it comes to the charging habit. The fast charging is performed with high power when the battery state of charge is low and the power decreases as the state of charge increases. This makes it more time effective to charge from 10 to 30% state of charge than from 50 to 70% because of the different output powers. The habit to charge the battery from and to a certain state of charge should also be of interest. This habit can be of importance when the capacity of the battery is considered. In other words if the fully range of the battery is used or not. If the fully range is not used, then a smaller battery pack can be installed to save cost and weight of the vehicle.

A future scenario could be, to make it possible to switch from fast charging to normal charging during the charging process. The advantage would be to gain an higher efficiency, to the cost of a longer charging time. By considering the amount of future customer, it may not be so efficient to increase the charging time. The longer charging time, the more charging stations are needed, which leads to higher investment costs. As mention in this study the Combo standard has both the DC and AC pins in the same connector. By using the Combo standard it would be possible to switch from DC fast charging to the AC charging without connecting two connectors to the vehicle. The only remaining limitation is to make the software compatible, so the changeover could take place in a safe manner both regarding the user and the equipment.

Many details remains to achieve an optimal fast charging station, but the prototype station is fully capable to charge EV:s. Experience during this study shows that the major limitation for the prototype is the heat generation, which implies the necessity of an air ventilation. Otherwise there is a risk of overheating the fast charging station, which leads to an automatically shut down. Since the study has not been performed during high ambient temperature, it is an future factor that must be evaluated.

An effect of improved infrastructure for fast charging possibilities is to evaluate the capacity of the power grid. Therefore simulations on the presence of several charging stations in one area must be considered, to see how the grid is affected and what actions are needed to be taken.

References

[1] ABB. “Snabb laddning ska få fart på Green Highway”. In: *Minimedia* (2012-05-26).

[2] ABB. *Terra 51 Charging Station product description*. 2012.

[3] D. Aggeler et al. “Ultra-fast DC-charge infrastructures for EV-mobility and future smart grids”. In: *Innovative Smart Grid Technologies Conference Europe (ISGT Europe)*. IEEE PES. 2012.

[4] American Physical Society. “Lithium-ion batteries”. In: (2012). URL: `http://physicscentral.org/explore/action/lithium-1.cfm`.

[5] CHAdeMO. *Interface*. Webpage. 2012.

[6] P. Pontice. *J1772 'combo connector' shown at the 2012 Electric Vehicle Symposium*. Automotive Engineer Online. http://www.sae.org/mags/aei/11005, 2012-05-03.

[7] Stockholm stad. “Snabbladdare i Bromma och Sätra”. In: (2012-05-23).

[8] Stockholms Stad and Vattenfall AB. “Tre nya snabbladdningsstationer har öppnat i Stockholm och Malmö”. In: (2012). URL: `http://www.elbilsupphandling.se/2012/04/tre-nya-snabbladdningsstationer-har-oppnat-i-stockholm-och-malmo/`.

[9] R. Klein et al. “Optimal Charging Strategies in Lithium-Ion Battery”. In: *American Control Conference (ACC)*. 2011.

[10] L. Spante. *Fast Charging Stations Market situation and Installation guidelines*. Tech. rep. Vattenfall, Asset Development, E-mobility R&D Program. Vattenfall Research and Development AB, 2011.

[11] Yokogawa Meters and Instruments Corporation, ed. *WT1800 Precision Power Analyzer Gettting Started Guide*. 2011.

[12] ZERO Zero Emission Resoruce Organisation. *Taking charge - Introducing fast chargers in Norway*. booklet. 2011.

[13] D. ZHANG, Y. MA, and Q.-W. BAI. *Estimation of Lithium-ion Battery State of Charge*. 2011.

[14] T. Anegawa. *Safety Design of CHAdeMO Quick Charger and its impact on Power Grid*. Presentation. TEPCO. 2010.

[15] C. Botsford and A. Szczepanek. “Fast Charging vs. Slow Charging: Pros and cons for the New Age of Electric Vehicles”. In: *EVS24 International Battery, Hybrid and Fuel Cell Electric Vehicle Symposium*. 2009.

[16] D. B. Sandalow. *Plug-In Electric Vehicles: What Role for Washington?* The Brookings Institution, 2009.

[17] Sustainable Energy Irland. *Hybrid Electric and Battery Electric Vehicles Byers Guide*. booklet. 2007.

[18] Svenska Kraftnät. *Tekniska riktlinjer för elkvalitet Del 1: Spänningens egenskaper i stamnätet*. Tech. rep. TR6-01 rev B. Jan. 2006.

[19] S.-E. Berglund and J. Åkerlund. *EMC, elkvalitet och elmiljö*. Tech. rep. 2004-40. Elforsk, 2004.

[20] SIS Swedish Standards Institute. *SS-EN 61000-2-2 Electromagnetic compatibility (EMC) - Part 2-2: Environment - Compatibility levels for low-frequency conducted disturbances and signalling in public low-voltage power supply systems*. 2003.

[21] M. Bojrup et al. “A Dual Purpose Battery Charger for Electric Vehicles”. In: *Power Electronics Specialists Conference, . PESC 98 Record*. Department of Industrial Electrical Engineering and Automation Lund Institute of Technology. 29th Annual IEEE, 1998.

[22] P. Karlsson et al. *Efficiency of Off-Board, High Power, Electric Vehicle Battery Chargers With Active Power Line Conditioning Capabilities*. Tech. rep. Department of Industrial Electrical Engineering and Automation, Lund Institute of Technology, 1997.
[23] Citroën. *Citroën C-Zero brochure*. booklet.
[24] Fluke, ed. *80i-500s Current probe for oscilloscopes*.
[25] M. Goldmann. *Car test: Citroën C-Zero*. booklet. Gröna Bilister.
[26] LEM Probes, ed. *Current probe model PR2000*.
[27] P. Svedberg. *HRM Engineering*.

A Appendix

A.1 Matlab code for importing data

A.1.1 Importing Yokogawa measurement file

```
clear all; clc; close all;format compact;
tic
\%Lists all folders beginning with 2012
paths = dir('2012*');
for j = 1:size(paths, 1)
    currentPath = paths(j, 1).name
    \% Lists all csv-files in subfolder Yokogawa
    filenames = dir(fullfile(cd, paths(j, 1).name, 'Yokogawa', '*.csv'));
    for i = 1:size(filenames, 1)
        filename = filenames(i, 1).name;
        name = filename(1:strfind(filename, '.')-1);
        idx = strfind(paths(j, 1).name, ' ');
        measurement = paths(j, 1).name(idx(1)+1:idx(2)-1);

        fid = fopen(fullfile(cd, paths(j, 1).name, 'Yokogawa', filename));

        tline = fgetl(fid);
        dataHeader = regexp(tline, ', ', 'split');
        k = 1;
        while ischar(tline)
            tline = fgetl(fid);
            if size(tline, 2) > 10
                data(k, :) = str2double(regexp(tline, ', ', 'split'));
                k = k+1;
            end;
        end;

        evalin('base', [measurement, '_', name, '_data = data;']);
        evalin('base', [measurement, '_', name, '_dataHeader = dataHeader;']);
        clear data;clear data Header;
        [measurement '_' name]
        toc
    end;
end;
save(strcat(measurement, '_Yokogawa'), '-regexp', strcat('^',
```

```
    measurement));
clear all;
```

A.1.2 Importing CAN data file

```
clear all; clc; close all;format compact;
\%Lists all folders beginning with 2012
paths = dir('2012*');
for j = 1:size(paths, 1)
    tic
    paths(j, 1).name
    \% Lists all csv-files in subfolder CAN
    filenames = dir(fullfile(cd, paths(j, 1).name, 'CAN',
        '*.asc'));
    idx = strfind(paths(j, 1).name, ' ');
    measurement = paths(j, 1).name(idx(1)+1:idx(2)-1);
    for i = 1:size(filenames, 1)
        filename = filenames(i, 1).name
        name = filename(1:strfind(filename, '.')-1);
        fid = fopen(fullfile(cd, paths(j, 1).name, 'CAN',
            filename));
        A = textscan(fid, '%f %u %s Rx d %u %s %s %s %s %s %s %s
            %s %s %s', 'HeaderLines', 13);
        fclose(fid);clear fid;
        can(:, 1) = A{1, 1};
        can(:, 2) = A{1, 2};
        can(:, 3) = hex2dec(A{1, 3});
        can(:, 4) = A{1, 4};
        for k = 5:12
            can(:, k) = hex2dec(A{1, k});
        end;

        evalin('base', [measurement, '_', name, '_data = can;']);
        evalin('base', [measurement, '_', name, '_id =
            unique(sort(can(:, 3)));']);
        clear can;
        [measurement name]
        toc
    end;
end;
save(fullfile(cd, '_matlab', strcat(measurement, '_can')),
    '-regexp', strcat('^', measurement));
clear all;
```

A.2 Matlab code for scaling and viewing measurement

A.2.1 Main program

```
clear all;close all;clc; format compact;
clear('-regexp', '^(car|cha|bat|elc)');
measurement_all = {'ABB1', 'ABB2', 'ABB3', 'ABB5', 'ABB7',
    'ABB8', 'SLOW2'};
can = true; \%Scale can data
for n = 1:size(measurement_all, 2)
    measurement = measurement_all{i}

    evalin('base', [measurement '_elc = load(''' fullfile(cd,
        'mat', [measurement '_Yokogawa']) ''');']);
    if can
        evalin('base', [measurement '_can = load(''' fullfile(cd,
            'mat', [measurement '_can']) ''');']);
    end;

    createElcCarBatCha;
    if strcmp(measurement, 'SLOW2')
        elc{n}(:, 2) = ((0:0.5:(size(elc{i}, 1)-1)*0.5))';
    else
        elc{n}(:, 2) = ((0:0.05:(size(elc{i}, 1)-1)*0.05))';
    end
end;
nameAndScaleData;
nameAndScaleBat
plotAll;
```

A.2.2 Combine files (createElcCarBatCha.m)

```

% Select can-data files
tic;

elc{n} = NaN(1, 1234);
car{n} = NaN(1, 12);
cha{n} = NaN(1, 12);
bat{n} = NaN(1, 12);

switch measurement
    case 'ABB1'
        elc{n} = [
            NaN(6.1/0.05, 1234);
            ABB1_elc.ABB1_20120321_120855_data;
```

```
            NaN(65/0.05, 1234);
            ABB1_elc.ABB1_20120321_121311_data;
            NaN(203.05/0.05, 1234);
            ABB1_elc.ABB1_20120321_123902_data
            ];
        if can
            car{n} = ABB1_can.ABB1_car002_data;
            car{n}(:, 1) = car{n}(:, 1)+2000;
            car{n} = [ABB1_can.ABB1_car001_data;car{n}];
            %car(:, 1) = car(:, 1);

            bat{n} = ABB1_can.ABB1_bat002_data;
            bat{n}(:, 1) = bat{n}(:, 1)+2000;
            bat{n} = [ABB1_can.ABB1_bat001_data;bat{n}];
            %bat(:, 1) = bat(:, 1)+60.5;

            cha{n} = ABB1_can.ABB1_charge002_data;
            cha{n}(:, 1) = cha{n}(:, 1)+1847.7;
            cha{n} = [ABB1_can.ABB1_charge001_data;cha{n}];
            cha{n}(:, 1) = cha{n}(:, 1)+173.1;
        end
    case 'ABB2'
        elc{n} = [
            NaN(15.55/0.05, 1234);
            ABB2_elc.ABB2_20120402_110830_data;
            NaN(8.6/0.05, 1234);
            ABB2_elc.ABB2_20120402_114155_data
            ];
        if can
            car{n} = ABB2_can.ABB2_car001_data;

            bat{n} = ABB2_can.ABB2_bat001_data;
            bat{n}(:, 1) = bat{n}(:, 1)+282;

            cha{n} = ABB2_can.ABB2_charge001_data;
            cha{n}(:, 1) = cha{n}(:, 1) + 284.943;
        end
    case 'ABB3'
        elc{n} = [
            ABB3_elc.ABB3_20120403_071049_data;
            NaN(0.85/0.05, 1234);
            ABB3_elc.ABB3_20120403_081735_data;
            NaN(334/0.05, 1234);
            ABB3_elc.ABB3_20120403_083802_data;
            ];
        if can
```

```
            car{n} = ABB3_can.ABB3_car003_data;
            car{n}(:, 1) = car{n}(:, 1)+5500;
            car{n} = [ABB3_can.ABB3_car001_data;car{n}];

            bat{n} = ABB3_can.ABB3_bat003_data;
            bat{n}(:, 1) = bat{n}(:, 1)+5500;
            bat{n} = [ABB3_can.ABB3_bat001_data;bat{n}];
            %bat(:, 1) = bat(:, 1);

            cha{n} = ABB3_can.ABB3_charge003_data;
            cha{n}(:, 1) = cha{n}(:, 1)+5500+25.85;
            cha{n} = [ABB3_can.ABB3_charge001_data;cha{n}];
            cha{n}(:, 1) = cha{n}(:, 1)+12.3;
        end
    case 'ABB4'
        elc{n} = NaN(1, 1234);
        if can
            car{n} = ABB4_can.ABB4_car001_data;

            bat{n} = ABB4_can.ABB4_bat001_data;
            bat{n}(:, 1) = bat{n}(:, 1);

            cha{n} = ABB4_can.ABB4_charge001_data;
            cha{n}(:, 1) = cha{n}(:, 1) + 12.733;
        end
    case 'ABB5'
        elc{n} = [
            %NaN(3.25/0.05, 1234);
            ABB5_elc.ABB5_20120405_065431_data(62:67863, :);
            NaN(3.45/0.05, 1234);
            ABB5_elc.ABB5_20120405_075108_data
            ];
        if can
            car{n} = ABB5_can.ABB5_car001_data;
            bat{n} = ABB5_can.ABB5_bat001_data;
            cha{n} = ABB5_can.ABB5_charge001_data;
            cha{n}(:, 1) = cha{n}(:, 1)+62.636;
        end
    case 'ABB6'
        elc{n} = [NaN(8.4/0.05, 1234);
            ABB6_elc.ABB6_20120503_103552_data];
        if can
            car{n} = ABB6_can.ABB6_car001_data;
            cha{n} = ABB6_can.ABB6_charge001_data;
        end
    case 'ABB7'
```

```
            elc{n} = [NaN(2.3/0.05, 1234);
                ABB7_elc.ABB7_20120504_081229_data
                NaN(6.35/0.05, 1234);
                ABB7_elc.ABB7_20120504_083445_data];
            if can
                car{n} = ABB7_can.ABB7_car001_data;
                cha{n} = ABB7_can.ABB7_charge001_data;
            end
        case 'ABB8'
            elc{n} = [NaN(1.1/0.05, 1234);
                ABB8_elc.ABB8_20120523_112613_data
                NaN(3.1/0.05, 1234);
                ABB8_elc.ABB8_20120523_114531_data];
            if can
                car{n} = ABB8_can.ABB8_car001_data;
                cha{n} = ABB8_can.ABB8_charge001_data;
            end
        case 'SLOW2'
                elc{n} = SLOW2_elc.SLOW2_20120524_151636_data;
            if can
                car{n} = SLOW2_can.SLOW2_car001_data;
            end
        case 'Check'
            car{n} = Check_car001_data;
            car{n}(:, 1) = car{n}(:, 1)+50000;
            car{n} = [Check_car000_data;car{n}];
        otherwise
end
toc;
```

A.2.3 Assign and scale data (nameAndScaleData.m)

```
clear('-regexp', '^(car|cha|bat|elc)[a-zA-Z0-9]');
tic;
elcU1{n} = [elc{n}(:,2) elc{n}(:,4)];
elcU2{n} = [elc{n}(:,2) elc{n}(:,40)];
elcU3{n} = [elc{n}(:,2) elc{n}(:,76)];
elcU4{n} = [elc{n}(:,2) elc{n}(:,112)];
elcUA{n} = [elc{n}(:,2) elc{n}(:,184)];

elcI1{n} = [elc{n}(:,2) elc{n}(:,9)];
elcI2{n} = [elc{n}(:,2) elc{n}(:,45)];
elcI3{n} = [elc{n}(:,2) elc{n}(:,81)];
elcI4{n} = [elc{n}(:,2) elc{n}(:,117)];
elcIA{n} = [elc{n}(:,2) elc{n}(:,189)];

elcPA{n} = [elc{n}(:,2) elc{n}(:,194)/1e3];
```

```
elcSA{n} = [elc{n}(:,2) elc{n}(:,195)/1e3];
elcQA{n} = [elc{n}(:,2) elc{n}(:,196)/1e3];
elcP4{n} = [elc{n}(:,2) abs(elc{n}(:,122))/1e3];

elcP1{n} = [elc{n}(:,2) elc{n}(:,14)/1e3];
elcS1{n} = [elc{n}(:,2) elc{n}(:,15)/1e3];
elcQ1{n} = [elc{n}(:,2) elc{n}(:,16)/1e3];

elcNA{n} = [elc{n}(:,2) elc{n}(:,205)];
elcPFA{n} = [elc{n}(:,2) elc{n}(:,197)];

switch measurement
    case 'ABB1'
        soc{n}=17.5;
    case 'ABB2'
        soc{n}=10;
    case 'ABB3'
        soc{n}=10;
    case 'ABB4'
        soc{n}=9.5;
    case 'ABB5'
        soc{n}=9.5;
    case 'ABB6'
        soc{n}=9.5;
    case 'ABB7'
        soc{n}=43.5;
    case 'ABB8'
        soc{n}=50;
    case 'DBT1'
        soc{n}=0;
    case 'SLOW2'
        soc{n}=9.5;
    case 'Check2'
        soc{n}=37;
    otherwise
        soc{n}=0;
end;

socScale = 0.160;

elcE4{n} = [elc{n}(:,2) (elc{n}(:,142)/160+soc{n})*socScale];
elcEA{n} = [elc{n}(:,2) (elc{n}(:,203)/160+soc{n})*socScale];
elcE1{n} = [elc{n}(:,2) (elc{n}(:,34)/160+soc{n})*socScale];

%% Name and scale can data

```

```
%% Chademo
M=cha{n}(ismember(cha{n}(:,3),257),:);
 chaO0257new1{n} = [M(:,1) M(:,4+2)];
 chaO0257new2{n} = [M(:,1) M(:,4+3)];

M=cha{n}(ismember(cha{n}(:,3),258),:);
 chaE0258soc{n} = [M(:,1) M(:,4+7)*(1/1.5)*socScale];
 chaI0258current{n} = [M(:,1) M(:,4+4)];

M=cha{n}(ismember(cha{n}(:,3),265),:);
 chaU0265voltage{n} = [M(:,1) M(:,4+3)*255+M(:,4+2)];
 chaI0265current{n} = [M(:,1) M(:,4+4)];
 chaX0265new1{n} = [M(:,1) M(:,4+6)];
 chaX0265new2{n} = [M(:,1) M(:,7+4)+M(:,8+4)]; % Look again


%% Car
M=car{n}(ismember(car{n}(:,3),646),:);
 carF0646new{n} = [M(:,1) M(:,4+4)*2];

M=car{n}(ismember(car{n}(:,3),648),:);
 carU0648voltageLow{n} = [M(:,1) M(:,4+5)*2];

M=car{n}(ismember(car{n}(:,3),664),:);
 carT0664cabinTemp1{n} = [M(:,1) M(:,4+1)-40];
 carT0664ambientTemp1{n} = [M(:,1) M(:,4+2)-40];
 carT0664batteryTemp{n} = [M(:,1) M(:,4+3)-40];
 carT0664ambientTemp2{n} = [M(:,1) M(:,4+4)-40];

M=car{n}(ismember(car{n}(:,3),838),:);
 carE0838socDisplay{n} = [M(:,1) M(:,4+3)*socScale];

M=car{n}(ismember(car{n}(:,3),883),:);
 carU0883voltagePack1{n} = [M(:,1) M(:,4+1)];
 carU0883voltagePack2{n} = [M(:,1) M(:,4+2)];
 carI0883currentHighRes{n} = [M(:,1) ((M(:,4+3)*255+M(:,4+4))-2^15+255)*0.01];
 carU0883voltageHighRes{n} = [M(:,1) (M(:,4+5)*255+M(:,4+6))*0.1];
 carP0883powerCalculated{n} = [M(:,1) ( carI0883currentHighRes{n}(:,2).* carU0883voltageHighRes{n}(:,2) )/1e3];
 carE0883energyCalculated{n} = [M(:,1) ( cumsum( carP0883powerCalculated{n}(:,2)*1e3*0.01,1 )/3600/160 + soc{n})*socScale];

M=car{n}(ismember(car{n}(:,3),884),:);
```

```
carE0884socMin{n} = [M(:,1) (M(:,4+1)*0.5-5)*socScale];
carE0884socMax{n} = [M(:,1) (M(:,4+2)*0.5-5)*socScale];
carI0884currentLimitationLow{n} = [M(:,1) M(:,4+3)];
carI0884currentLimitationHigh{n} = [M(:,1) M(:,4+4)];
carT0884batteryMaxTemp{n} = [M(:,1) M(:,4+5)-40];
carT0884batteryMinTemp{n} = [M(:,1) M(:,4+6)-40];

M=car{n}(ismember(car{n}(:,3),900),:);
carF0900temp1{n} = [M(:,1) M(:,4+6)];
carF0900temp2{n} = [M(:,1) M(:,4+7)];

M=car{n}(ismember(car{n}(:,3),1685),:);
carV1685new1{n} = [M(:,1) M(:,4+1)*255+M(:,4+2)];
carV1685new2{n} = [M(:,1) M(:,4+4)*255+M(:,4+5)];


M=car{n}(ismember(car{n}(:,3),1686),:);
carV1686new2{n} = [M(:,1) M(:,4+1)*255+M(:,4+2)];
carV1686new3{n} = [M(:,1) M(:,4+3)*255+M(:,4+4)];

M=car{n}(ismember(car{n}(:,3),1687),:);
carU1687voltage{n} = [M(:,1) M(:,4+1)*255+M(:,4+2)];
carI1687current1{n} = [M(:,1) M(:,4+3)];
carI1687current2{n} = [M(:,1) M(:,4+7)];

M=car{n}(ismember(car{n}(:,3),1761),:);
carW1761batteryMaxTempPWM{n} = [M(:,1) M(:,4+3)-40];
carW1761batteryMinTempPWM{n} = [M(:,1) M(:,4+4)-40];
carV1761voltage5{n} = [M(:,1) M(:,4+5)*255+M(:,4+6)];
carV1761voltage7{n} = [M(:,1) M(:,4+7)*255+M(:,4+8)];

M=car{n}(ismember(car{n}(:,3),1762),:);
carW1762batteryAverageTempPWM{n} = [M(:,1) M(:,4+2)-40];
carV1762voltage5{n} = [M(:,1) M(:,4+5)*255+M(:,4+6)];
carV1762voltage7{n} = [M(:,1) M(:,4+7)*255+M(:,4+8)];

M=car{n}(ismember(car{n}(:,3),1763),:);
carY1763new2{n} = [M(:,1) M(:,4+2)-40];
carY1763new3{n} = [M(:,1) M(:,4+3)];

M=car{n}(ismember(car{n}(:,3),1882),:);
carT1882ambientTemp1{n} = [M(:,1) M(:,4+7)-40];
carT1882ambientTemp2{n} = [M(:,1) M(:,4+8)-40];

M=car{n}(ismember(car{n}(:,3),1883),:);
carT1883cabinTemp1{n} = [M(:,1) M(:,4+1)-40];
```

```
carT1883cabinTemp2{n} = [M(:,1) M(:,4+2)-40];
carT1883cabinTemp3{n} = [M(:,1) M(:,4+3)-40];
carT1883batteryTemp{n} = [M(:,1) M(:,4+4)-40];
carV1883new6{n} = [M(:,1) M(:,4+6)];

%Derivate state of charge
M = [round(carE0884socMin{n}(:,2)/socScale*10) carE0884socMin{n}(:,1)];
M(all(M(:,1)<1,2),:)=[];
M=[
    accumarray(M(:,1),M(:,2),[],@(x)min(x)) ...     %Time
    accumarray(M(:,1),M(:,1),[],@(x)min(x))/10        %SOC
    ];
M(all(M==0,2),:)=[];
carP0884fromSOCmin{n} = [M(1:size(M,1)-1,1) 3600*160*diff(M(:,2))./diff(M(:,1))/1e3];

M = [round(carE0884socMax{n}(:,2)/socScale*10) carE0884socMax{n}(:,1)];
M(all(M(:,1)<1,2),:)=[];

M=[
    accumarray(M(:,1),M(:,2),[],@(x)min(x)) ...
    accumarray(M(:,1),M(:,1),[],@(x)min(x))/10
    ];
M(all(M==0,2),:)=[];
carP0884fromSOCmax{n} = [M(1:size(M,1)-1,1) 3600*160*diff(M(:,2))./diff(M(:,1))/1e3];

M = [round(chaE0258soc{n}(:,2)/socScale/10) chaE0258soc{n}(:,1)];
M(all(M(:,1)<1,2),:)=[];

M=[
    accumarray(M(:,1),M(:,2),[],@(x)min(x)) ...
    accumarray(M(:,1),M(:,1),[],@(x)min(x))*10
    ];
M(all(M==0,2),:)=[];
chaP0258fromSoc{n} = [M(1:size(M,1)-1,1) 3600*160*diff(M(:,2))./diff(M(:,1))/1e3];

%% Bat
if exist('bat','var')
    M=bat{n}(ismember(bat{n}(:,3),963),:);
    batU0963AverangeCellVoltage{n} = [M(:,1) (M(:,4+1)*255+M(:,4+2))*0.01];
end
```

```
toc;

end;
```

A.2.4 Assign and scale battery CAN data (nameAndScaleBat.m)

```
moduleID = [1553 1569 1585 1601 1617 1633 1649 1665 1681 1697 1713 1729]';

m1 = [
    'C' 'B' 'T' 'T' 'V' '-' 'V' '-';
    'C' 'T' 'T' 'B' 'V' '-' 'V' '-';
    'C' 'T' 'T' 'B' 'V' '-' 'V' '-';
    'C' 'B' 'B' 'B' 'V' '-' 'V' '-'];

m6 = [
    'C' 'B' 'T' 'T' 'V' '-' 'V' '-';
    'C' 'T' 'O' 'B' 'V' '-' 'V' '-';
    'C' 'O' 'O' 'B' 'O' 'O' 'O' 'O';
    'C' 'B' 'B' 'B' 'O' 'O' 'O' 'O'];

moduleM = {m1 m1 m1 m1 m1 m6 m1 m1 m1 m1 m1 m6}';

for i = 1:size(moduleID, 1)
    for j = 0:3
        M = bat{n}(ismember(bat{n}(:, 3), moduleID+j), :);
        for k = 1:8
            switch moduleM{n}(j+1, k)
                case 'V'
                    evalin('base', sprintf('bat%02iU%0icellVoltage%i = [M(:, 1) (M(:, %i)*255+M(:, %i))*0.01];', i, moduleID(i)+j, k, 4+k, 4+k+1));
                case 'T'
                    evalin('base', sprintf('bat%02iU%0icellTemperature%i = [M(:, 1) M(:, %i)-40];', i, moduleID(i)+j, k, 4+k));
                case 'B'
                    evalin('base', sprintf('bat%02iU%0icellBalance%i = [M(:, 1) M(:, %i)];', i, moduleID(i)+j, k, 4+k));
                case 'O'
                    evalin('base', sprintf('bat%02iU%0icellUnknowed%i = [M(:, 1) M(:, %i)];', i, moduleID(i)+j,
```

```
                    k, 4+k));
                otherwise
            end;
        end;
    end;
end;
```

A.2.5 Plot data (plotAll.m)

```
clear vars;
close all;
names = {'Energy', 'Current', 'Voltage', 'Power', 'TempCabin',
    'TempBattery'};
vars{1} = [who('*E*')];
vars{2} = [who('chaI*');who('carI*');who('elcI4*');who('elcI1*')];
vars{3} = [who('carU*');who('chaU*');who('elcU4*');who('elcU1*')];
vars{2} = [who('carP*');who('elcPA');who('elcP4');who('chaP*')];
vars{4} = [who('carT*ambient*')];
vars{5} = [who('carT*cabin*')];
vars{6} = [who('carT*battery*')];%who('bat*Temp*');

color = ['k';'b';'r';'g';'c';'m';'y'];
lines = ['- ';': ';'--';'.-';'- ';': ';'--';'.-'];

type = ['+' 'o' '*' '.' 'x' 's' 'd' '^' 'v' '<' '>' 'p' 'h'];

for i = 1:size(vars, 2)
    for k = 2:2%size(measurement_all, 2)
        if ~strcmp(measurement_all(k), 'O')
            h = figure('Name', sprintf('%s %s', names{i},
                measurement_all{k}), 'NumberTitle', 'off');
            %subplot(1, size(measurement_all, 2), k)
            title(measurement_all(k));
            for j = 1:size(vars{i}, 1)
                p = evalin('base', ['not(isempty(' vars{i}{j, :}
                    '{k}))']);
                if p
                    evalin('base', ['plot(', vars{i}{j, 1},
                        '{k}(:, 1), ', vars{i}{j, 1}, '{k}(:, 2),
                        ''' color(mod(j, 7)+1)
                        '.'')']);%type(mod(i, 13)+1)
                        lines(ceil(j/7), :)
                else
                    evalin('base', ['plot([0 0], [0 0], '''
                        color(mod(j, 7)+1) lines(ceil(j/7), :)
                        ''')']);
                end
```

```
                    hold on;
                end;
                legend(vars{i}{:, 1});
                set(gcf, 'PaperUnits', 'inches', 'PaperPosition', [0
                    0 10 10]);
                print('-dpng', fullfile(cd, 'png', sprintf('%s %s',
                    names{i}, measurement_all{k})));
                saveas(h, fullfile(cd, 'fig', sprintf('%s %s',
                    names{i}, measurement_all{k})), 'fig');
            end;
        end;
end;
```